

REPORT DOCUMENTATION PAGE

Form Approved
OMB No. 0704-0188

Public reporting burden for this collection of information is estimated to average 1 hour per response, including the time for reviewing instructions, searching existing data sources, gathering and maintaining the data needed, and completing and reviewing the collection of information. Send comments regarding this burden estimate or any other aspect of this collection of information, including suggestions for reducing this burden, to Washington Headquarters Services, Directorate for Information Operations and Reports, 1215 Jefferson Davis Highway, Suite 1204, Arlington, VA 22202-4302, and to the Office of Management and Budget, Paperwork Reduction Project (0704-0188), Washington, DC 20503.

1. AGENCY USE ONLY (Leave blank)		2. REPORT DATE <i>9 Dec 96</i>	3. REPORT TYPE AND DATES COVERED	
4. TITLE AND SUBTITLE <i>A Finite Element Model for Harmonic Response of a Viscoelastic Sandwich Beam.</i>			5. FUNDING NUMBERS	
6. AUTHOR(S) <i>Richard Allen Maddox.</i>				
7. PERFORMING ORGANIZATION NAME(S) AND ADDRESS(ES) <i>University of Virginia</i>			8. PERFORMING ORGANIZATION REPORT NUMBER <i>96-088</i>	
9. SPONSORING / MONITORING AGENCY NAME(S) AND ADDRESS(ES) DEPARTMENT OF THE AIR FORCE AFIT/CI 2950 P STEET, BLDG 125 WRIGHT-PATTERSON AFB OH 45433-7765			10. SPONSORING / MONITORING AGENCY REPORT NUMBER	
11. SUPPLEMENTARY NOTES				
12a. DISTRIBUTION / AVAILABILITY STATEMENT <i>Unlimited</i>			12b. DISTRIBUTION CODE	
13. ABSTRACT (Maximum 200 words)				
14. SUBJECT TERMS			15. NUMBER OF PAGES <i>52+</i>	
			16. PRICE CODE	
17. SECURITY CLASSIFICATION OF REPORT	18. SECURITY CLASSIFICATION OF THIS PAGE	19. SECURITY CLASSIFICATION OF ABSTRACT	20. LIMITATION OF ABSTRACT	

GENERAL INSTRUCTIONS FOR COMPLETING SF 298

The Report Documentation Page (RDP) is used in announcing and cataloging reports. It is important that this information be consistent with the rest of the report, particularly the cover and title page. Instructions for filling in each block of the form follow. It is important to *stay within the lines* to meet *optical scanning requirements*.

Block 1. Agency Use Only (Leave blank).

Block 2. Report Date. Full publication date including day, month, and year, if available (e.g. 1 Jan 88). Must cite at least the year.

Block 3. Type of Report and Dates Covered. State whether report is interim, final, etc. If applicable, enter inclusive report dates (e.g. 10 Jun 87 - 30 Jun 88).

Block 4. Title and Subtitle. A title is taken from the part of the report that provides the most meaningful and complete information. When a report is prepared in more than one volume, repeat the primary title, add volume number, and include subtitle for the specific volume. On classified documents enter the title classification in parentheses.

Block 5. Funding Numbers. To include contract and grant numbers; may include program element number(s), project number(s), task number(s), and work unit number(s). Use the following labels:

C - Contract	PR - Project
G - Grant	TA - Task
PE - Program Element	WU - Work Unit Accession No.

Block 6. Author(s). Name(s) of person(s) responsible for writing the report, performing the research, or credited with the content of the report. If editor or compiler, this should follow the name(s).

Block 7. Performing Organization Name(s) and Address(es). Self-explanatory.

Block 8. Performing Organization Report Number. Enter the unique alphanumeric report number(s) assigned by the organization performing the report.

Block 9. Sponsoring/Monitoring Agency Name(s) and Address(es). Self-explanatory.

Block 10. Sponsoring/Monitoring Agency Report Number. (If known)

Block 11. Supplementary Notes. Enter information not included elsewhere such as: Prepared in cooperation with...; Trans. of...; To be published in.... When a report is revised, include a statement whether the new report supersedes or supplements the older report.

Block 12a. Distribution/Availability Statement. Denotes public availability or limitations. Cite any availability to the public. Enter additional limitations or special markings in all capitals (e.g. NOFORN, REL, ITAR).

DOD - See DoDD 5230.24, "Distribution Statements on Technical Documents."

DOE - See authorities.

NASA - See Handbook NHB 2200.2.

NTIS - Leave blank.

Block 12b. Distribution Code.

DOD - Leave blank.

DOE - Enter DOE distribution categories from the Standard Distribution for Unclassified Scientific and Technical Reports.

NASA - Leave blank.

NTIS - Leave blank.

Block 13. Abstract. Include a brief (*Maximum 200 words*) factual summary of the most significant information contained in the report.

Block 14. Subject Terms. Keywords or phrases identifying major subjects in the report.

Block 15. Number of Pages. Enter the total number of pages.

Block 16. Price Code. Enter appropriate price code (*NTIS only*).

Blocks 17. - 19. Security Classifications. Self-explanatory. Enter U.S. Security Classification in accordance with U.S. Security Regulations (i.e., UNCLASSIFIED). If form contains classified information, stamp classification on the top and bottom of the page.

Block 20. Limitation of Abstract. This block must be completed to assign a limitation to the abstract. Enter either UL (unlimited) or SAR (same as report). An entry in this block is necessary if the abstract is to be limited. If blank, the abstract is assumed to be unlimited.

**A Finite Element Model for Harmonic Response of a
Viscoelastic Sandwich Beam**

A Thesis

Presented to
The Faculty of the
School of Engineering and Applied Science
University of Virginia

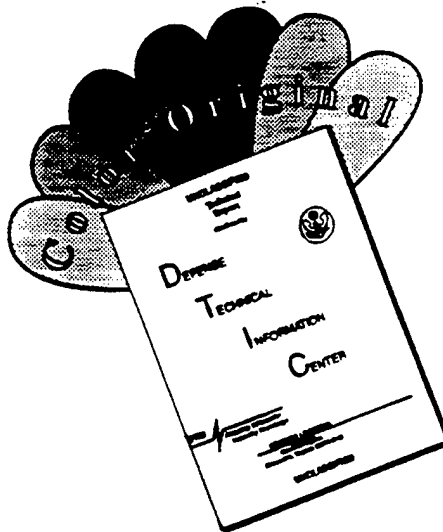
In Partial Fulfillment
of the Requirements for the Degree
Master of Science in Civil Engineering

by

Richard Allen Maddox
May 1996

19961212 021

DISCLAIMER NOTICE

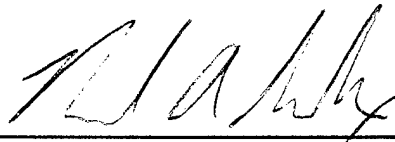


THIS DOCUMENT IS BEST QUALITY AVAILABLE. THE COPY FURNISHED TO DTIC CONTAINED A SIGNIFICANT NUMBER OF COLOR PAGES WHICH DO NOT REPRODUCE LEGIBLY ON BLACK AND WHITE MICROFICHE.

APPROVAL SHEET

The thesis is submitted in partial fulfillment of the
requirements for the degree of

Master of Science in Civil Engineering



Richard Allen Maddox

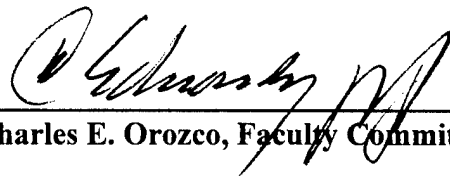
This thesis has been read and approved by the Examining Committee:



Thomas T. Baber, Thesis Advisor



Furman W. Barton, Faculty Committee



Charles E. Orozco, Faculty Committee

Accepted for the School of Engineering and Applied Science:

**Dean, School of Engineering and
Applied Science**

May 1996

TABLE OF CONTENTS

	<u>Page</u>
LIST OF FIGURES	iii
LIST OF TABLES	iv
LIST OF SYMBOLS	v
ABSTRACT	vii
1. INTRODUCTION	1
1.1 Industrial Vibration Absorption	1
1.2 Sandwich Beams for TMD Applications	4
1.3 Viscoelasticity	5
2. SANDWICH BEAM MODELS	8
2.1 Single Variable Models	8
2.2 Multiple Variable Models	14
3. FINITE ELEMENT FORMULATION FOR DAMPED SANDWICH BEAMS	24
3.1 Prior Research	24
3.2 Assumptions	26
3.3 Assuming Shape Functions	33
3.4 FORTRAN Program	38
3.5 Equation of Motion	38
3.6 FORTRAN Solution Process	39
4. NUMERICAL STUDIES	41
4.1 Test Cases	41
5. CONCLUSIONS	49
BIBLIOGRAPHY	51
APPENDICES	
1. Mass and Stiffness Matrices	A1
2. FORTRAN Program	A2
3. Ansys Program	A3

LIST OF FIGURES

#		<u>Page</u>
1	Typical Tuned Mass Damper	2
2	Beam-type TMD	3
3	Calculated depth, d , compared with Actual depth	12
4	Bai and Sun Shear Deformation, Ψ	15
5	Sandwich Beam Construction	15
6	Sandwich Beam Displacement Field	19
7	Reducing Displacement Field	20
8	Plot showing effect of core thickness on shear deformation, Ψ	32
9	1st Order Shape Functions	35
10	2nd Order Shape Functions	36
11	Displacement Vector	37
12	Specimen 1 Test Data	44
13	Lu and Douglas Test Data	45
14	Specimen 2 Test Data	46
15	Ansys Model	48

LIST OF TABLES

<u>#</u>		<u>Page</u>
1	Test Case Characteristics	42
2	Ansys Results	48

LIST OF SYMBOLS

a_{ij}	matrix element of the i th row, j th column
A	cross sectional area
c	viscous damping
d	depth of shear block
e	$2(1 + \nu_c)$
E	Young's modulus
E_c	complex Young's modulus of core
E_1	Young's modulus for top layer
E_2	Young's modulus for bottom layer
E^*	complex Young's modulus
f	natural frequency
\mathbf{F}	load vector
\mathbf{F}_0	harmonic loading vector
G	shear modulus
G_c	complex shear modulus of core
G^*	complex shear modulus
h	core layer thickness
h_1	top layer thickness
h_2	bottom layer thickness
i	square root of -1, element node
I	moment of inertia
Imp	driving point mechanical impedance
j	square root of -1, element node
k	stiffness, element node
k^*	complex stiffness
\mathbf{K}	stiffness matrix
\mathbf{K}^*	complex stiffness matrix
L	beam length
m	mass
M	cross sectional moment,
\mathbf{M}	mass matrix
N	shape function
p	transverse load
q	external load
Q	harmonic loading
S	sum of shear forces
t	time
T	Kinetic energy
u	longitudinal displacement

u^b	longitudinal displacement of bottom face
u_0	longitudinal displacement at centroid of core
u^c	longitudinal displacement of top face
u_1	longitudinal displacement of top layer at centroid
u_2	longitudinal displacement of bottom layer at centroid
\ddot{u}	longitudinal acceleration
\mathbf{U}	displacement vector, potential energy
$\ddot{\mathbf{U}}$	acceleration vector
w	transverse displacement
w^b	transverse displacement of bottom face
w^c	transverse displacement of core
w_0	transverse displacement at centroid of core
w^t	transverse displacement of top face
w_1	transverse displacement of top layer at centroid
w_2	transverse displacement of bottom layer at centroid
w_1'	rotation displacement of top face
w_2'	rotational displacement of bottom face
x	Cartesian coordinate
y	Cartesian coordinate
z	Cartesian coordinate
α	x dependent portion of longitudinal displacement, u
β	x dependent portion of transverse displacement, w
δ	damping factor
γ	shear strain
Φ	transverse normal deformation in core
ν	Poisson's ratio
ν_c	Poisson's ratio of core
ρ	mass/unit length
ρ_1	mass/unit length of top layer
ρ_2	mass/unit length of bottom layer
τ	shear force
ω	forcing frequency
Ω	forcing frequency
Ψ	shear deformation

ABSTRACT

After a discussion of the possible use of the sandwich beam design as a means of incorporating damping into tuned mass dampers, the development of a finite element model for viscoelastic sandwich beam analysis is presented.

The requirement for future use of the viscoelastic sandwich beam design in TMDs is to have a method by which the response of a beam with any given dimensions or end conditions can be determined. A survey of previous published research into sandwich beam behavior demonstrates the need for the finite element approach. The theory and assumptions presented in this previous research, provide the basis for the development of the approximation model presented here. A finite element model is presented that utilizes sandwich beam theory developed for thick damping layers. The model is constructed using standard beam and bar shape functions. Through an approximation introduced by observing the spatial variation of the core shear deformation, it was possible to eliminate all core variables and express the element behavior in terms of nodal displacements of the top and bottom face plates only. A FORTRAN computer program was written to perform the finite element analysis.

Using experimental data from previous research and data obtained through use of computer analysis software, results from this model are compared. The results are used to support the conclusion that this working model can be used in the future for the analysis of viscoelastic sandwich beams.

1.0 INTRODUCTION

1.1 Industrial Vibration Absorption

When industrial machinery is located within a structure, the resulting dynamic forces can have severe effects on the structure. The repetitive forces of many industrial machines may induce excessive floor vibrations. Over time the repeated back and forth deflection of floor members can cause fatigue and potential failure. If the frequency of the machinery coincides with the structure's natural frequency, the effects are most severe. In addition to possible damage to the structure, the machinery producing the disturbance moves with the floor to which it is attached. Therefore damage to or malfunction of the machine itself becomes a concern, especially in modern machinery containing sensitive computer components. An example of this occurred when the upgrade of machinery in one factory led to severe difficulties. The faster operating speeds of the new equipment induced a large vibration in the floor. In response to the motion of the floor, the machinery automatically shut itself down as a result of loss of alignment.

To improve a structure's behavior under periodic loading there are several alternatives. The structure can be stiffened to raise the resonant frequency, mass can be added to the structure to lower the resonant frequency, isolating pads can be used to reduce the transfer of energy from the machinery to the structure, or an energy absorbing device may be installed. Stiffening the structure or increasing its mass will shift its natural frequency out of the operating range of the machinery, but may require considerable modifications to the structure. This would mean increased costs to new construction and expensive alterations to an existing structure which may not be physically possible (Auerbach, 1995). The use of isolating pads can be beneficial, but will not always alleviate vibrations problems alone, especially when the vibrations are large.

For the purpose of absorbing vibrations, active and passive techniques can be employed which would dissipate the energy being applied to the structure thus reducing

the induced vibration. Passive devices tend to be more economical and reliable than active devices which depend upon intricate electronics. One technique for vibration control is that of installing tuned mass dampers (TMDs) on the structure. A TMD is a passive vibration absorber which dissipates a portion of the energy from a structure to which it is attached by vibrating independently of the structure. The natural frequency of the TMD is "tuned" (by design) to an optimum natural frequency allowing it to absorb the greatest amount of energy when the structure to which it is attached reaches resonance.

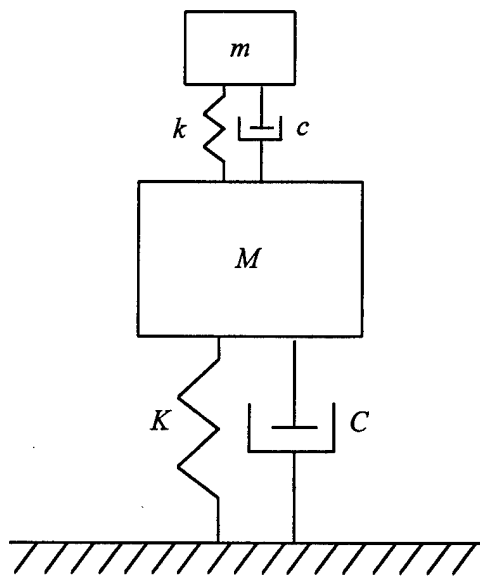


Figure 1 - Typical Tuned Mass Damper

TMDs are effectively used in mechanical engineering systems, including machinery, automotive and aircraft engines, and ships, and to reduce wind induced vibration of tall buildings and structures (Xu, Kwok, and Samali, 1992). The design of TMDs involves the consideration of its three components: mass, stiffness, and damping. The greater the mass of the TMD, the greater the amount of energy it will absorb. The amount of mass which can be used however is limited by practical concerns. Adding too much weight would require modification of the structure to support it. Size, cost, and constructability all dictate that the TMD's mass be small relative to the floor to which it is attached (Auerbach, 1995).

Since only small variations in the mass are possible, the stiffness of the TMD (represented as k in Figure 1) becomes critical in determining the natural frequency of the TMD. The required stiffness may be obtained in the design of the TMD through geometry, material composition, and connection methods. In general, increasing the stiffness of the TMD will decrease the amount of damping (represented as c in Figure 1) present and vice versa (Bai and Sun, 1995). The design of TMDs requires balancing these components to absorb the greatest amount of vibratory energy.

Specifically the device which this research is concerned with is the beam-type TMD. The use of a beam-type design allows for construction of a device which can attach easily to the floor system in a structure and would be compact enough to fit under the floor without major modifications to the structure. A beam-type TMD would be equipped with movable masses at each end for fine tuning the device during installation.

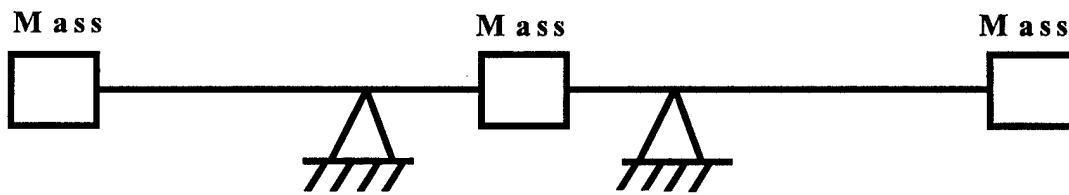


Figure 2 - Beam-type TMD

The disadvantage of the beam design is that the one mode of vibration possible in the lumped mass design in the Figure 1 is now increased to many possible modes. Careful

analysis must accompany any design to ensure that the proper mode of the beam-type TMD is excited.

Previous research at the University of Virginia has produced an optimal design method for beam-type TMDs. To test the accuracy of his design method, a beam-type TMD was constructed in the lab by Auerbach (1995). A model floor constructed by Sgambati (1994) was used as the platform for the experiment. Walsh (1994) added braces to the floor and determined the natural frequency and damping of the braced floor. Using this data, Auerbach was able to design a beam-type TMD for the braced floor. He constructed such a TMD and attached it under the floor system. As predicted, the TMD had the stiffness necessary to affect the floor's response to applied loads. What was missing however was the damping component of the TMD. Commercially made pneumatic dashpots and attaching butyl rubber strips to the outer faces of the TMD beam were able to provide a small amount of damping to the system. However, the optimal damping needed could not be reached.

1.2 Sandwich Beams for TMD Applications

The problem then becomes to develop a beam-type TMD which has stiffness to resist deflection and yet still provides damping of the vibration. For that purpose, this research was undertaken into the use of the sandwich beam design. Plantema (1966) defines sandwich construction as a layer type construction, consisting of thin sheets of high-strength material between which a thick layer of low average strength and density is sandwiched. Although multiple layers are possible, this research is only concerned with the simple three-layer sandwich beam. The two thin sheets are called the faces, and the intermediate layer is the core of the sandwich.

In the aerospace industry, where the use of sandwich construction is most prevalent mainly due to its weight savings and ease of mass production, the material of the faces may be aluminum alloy, reinforced plastic, titanium, heat-resistant steel, etc. For the core the material and the geometric shape can vary widely. Some of the main types of

cores used today are honeycomb cores, corrugated cores, balsa wood, and expanded materials such as cellulose acetate or synthetic rubber (Plantema, 1966).

1.3 Viscoelasticity

To achieve a high level of damping from the TMD, a core of viscoelastic material would be used. *Viscoelasticity* is the property of special materials such as rubber, which exhibit characteristics of being *viscous*, with stresses proportional to the rate of strain, and of being elastic, with stresses proportional to the strains. More generally, viscoelastic materials are those materials whose constitutive law relates the stresses and their time derivatives to the strains and their time derivatives.

When analyzing isotropic elastic materials, the relationships between stress and strain that a material exhibits can be represented by three values: the Young's modulus, E , the Shear modulus, G , and the Poisson's ratio, ν . For isotropic elastic materials where stresses are applied in-plane with the material (*plane stress*), the Young's modulus is related to the shear modulus by the following relationship:

$$G = \frac{E}{2(1 + \nu)} \quad [1]$$

The behavior of viscoelastic materials is not as simple to define as that of elastic material. As stress is applied to a viscoelastic material, it begins to deform elastically, but as the stress continues over time, there is a certain amount of mechanical loss in the material caused by the strain. For linearly viscoelastic materials, a general relationship between uniaxial stress and strain is given by the differential equation:

$$\left(a_0 + a_1 \frac{\partial}{\partial t} + a_2 \frac{\partial^2}{\partial t^2} + \dots + a_n \frac{\partial^n}{\partial t^n} \right) \sigma = \left(b_0 + b_1 \frac{\partial}{\partial t} + b_2 \frac{\partial^2}{\partial t^2} + \dots + b_p \frac{\partial^p}{\partial t^p} \right) \varepsilon \quad [2]$$

For general loading it is necessary to specify the response in terms of this differential equation, leading to a transient response.

In the case of response of a structure to harmonic excitation, a somewhat simpler approach is possible. One early researcher to use this approach was E.M. Kerwin Jr. (DiTaranto, 1965). If the excitation is taken in complex form as $F_0 e^{j\Omega t}$, then the stresses and strains may both be assumed to be of the same form. That is

$$\begin{aligned}\sigma &= \tilde{\sigma} e^{\Omega j t} \\ \varepsilon &= \tilde{\varepsilon} e^{\Omega j t}\end{aligned}\quad [3]$$

Substituting these equations into the differential constitutive equation [2], one obtains

$$[a_0 + j\Omega a_1 + (j\Omega)^2 a_2 + \dots + (j\Omega)^n a_n] \tilde{\sigma} = [b_0 + j\Omega b_1 + (j\Omega)^2 b_2 + \dots + (j\Omega)^p b_p] \tilde{\varepsilon}\quad [4]$$

This suggests that the stress-strain relationship under harmonic forcing may be expressed in the complex form

$$\tilde{\sigma} = E(1 + j\delta_E) \tilde{\varepsilon}\quad [5]$$

The analysis of viscoelastic materials under harmonic forcing therefore requires the use of complex moduli to represent both the elastic response of the material and the response due to the viscous dissipation of energy over time. The fact that the ratio of stress to strain is a complex quantity signifies that strain lags in phase behind stress by an angle the tangent of which is called the *loss or damping factor*. The resulting strain of viscoelastic material under a sufficiently small applied stress is a function of time alone and not of stress magnitude (Snowdon, 1968).

In many problems of interest much of the energy dissipation occurs in shear. following the above reasoning, Snowdon describes a *complex shear modulus*, G^* , to be used in the analysis of viscoelastic materials:

$$G^* = \text{complex shear modulus} = G (1 + j\delta) \quad [6]$$

where $j = \text{sq root of } -1$

$G =$ the dynamic shear modulus = is the real part of the modulus

$\delta =$ the loss or damping factor = is the ratio of the real part to the imaginary part

$G\delta =$ the imaginary part = is a measure of the mechanical loss associated with the shear deformation of the material

G^* and G are functions of temperature and of the angular frequency at which the stress and strain vary sinusoidally with time. As temperature decreases and as frequency increases the shear modulus increases. The increase continues towards a point where the dynamic modulus becomes so large that the characteristic resilience of a rubberlike material is no longer apparent. An inextensible (or glasslike) state is reached (Snowdon, 1968). This point is known as *transition* and the frequency and temperature at which this occurs is the transition frequency and the transition temperature. Viscoelastic material with a low transition frequency will have a maximum damping factor occurring at a low frequency. Those materials which produce high damping will have low transition frequencies. Examples of high damping viscoelastic materials are plasticized polyvinyl butyral resin, Thiokol RD, plasticized polyvinyl acetate, and butyl rubber (filled with 40 parts by weight of medium processing channel (MPC) black per 100 parts of rubber) (Snowdon, 1968).

Similar to the complex shear modulus is the complex Young's modulus:

$$E^* = \text{complex Young's modulus} = E (1 + j\delta) \quad [7]$$

The Poisson's ratio for viscoelastic materials approaches the perfectly elastic state for which the ratio is $1/2$. For calculations in this paper, a Poisson's ratio of 0.49 will be used. For purposes of this research, the complex Young's modulus is assumed to be related to the complex shear modulus by equation [1].

2.0 SANDWICH BEAM MODELS

2.1 Single Variable Models

Although the use of the viscoelastic sandwich beams have not been previously researched specifically for the use in tuned mass dampers, they have been the object of investigation in the reduction of the transmission of vibratory energy in structures and mechanical systems, especially in the aerospace industry, for many years.

One of the first attempts to formulate static and dynamic bending equations for viscoelastic sandwich beams was done in a paper by R.A. DiTaranto (1965). Using some basic assumptions set forth by Kerwin, DiTaranto was able to develop a sixth-order, complex, homogeneous differential equation for longitudinal displacements. He was then able to show how the solution of this equation, once boundary conditions were satisfied, would yield the natural frequencies and damping factors for viscoelastic sandwich beams.

The assumptions which DiTaranto followed were:

1. For the beam cross section, there is a neutral axis, whose location varies with frequency.
2. There is no slipping between the elastic and viscoelastic layers at their interfaces.
3. The major part of the damping is due to the shearing of the viscoelastic material.
4. The elastic layers displace laterally the same amount.
5. The beam is simply supported and vibrating at a natural frequency, or the beam is infinitely long so that the end effects may be neglected.
6. The normal forces acting in the core may be neglected in comparison to the normal forces in the elastic material.
7. Only transverse inertia is considered, the rotatory and longitudinal inertia of the beam are ignored.
8. The face plates are very stiff in shear. Therefore shear deformation of the face plates is neglected.

These assumptions allow for the closed form solution to the viscoelastic sandwich beam problem, but this has practical limitations since DiTaranto's equation is in terms of only the longitudinal displacements of the beam and is limited to simply supported end conditions. Although his equation is not directly applicable to boundary conditions other than simply supported, he was able to show that the relationship between the damping factor and the natural frequency is independent of the boundary conditions, but is dependent upon the cross-sectional geometry and the physical properties of the elastic and viscoelastic materials. Therefore the relationship which can be derived for the simply supported end condition will hold true for any other nondissipative boundary conditions.

Another limitation of the DiTaranto equation is the assumption that top and bottom faces always move transversely in-phase with one another ignores possible vibratory modes.

Although DiTaranto did not complete the substitution, it can be shown that the differential equation he solved is of the form:

$$\frac{B_1 + B_3}{R\delta} \frac{\partial^6 u_1}{\partial x^6} - \left[K_1\delta + (B_1 + B_3) \frac{S}{\delta} \right] \frac{\partial^4 u_1}{\partial x^4} = m \left[\frac{S}{\delta} \frac{\partial^2 u_1}{\partial t^2} - \frac{1}{R\delta} \frac{\partial^4 u_1}{\partial x^2 \partial t^2} \right] \quad [8]$$

where u_1 = longitudinal displacement of the top face layer's centroid

$$B_i = E_i I_i \quad i = 1, 3$$

$$K_i = E_i A_i \quad i = 1, 3$$

$$\delta = \frac{h_1}{2} + h_2 + \frac{h_3}{2} = d$$

$$S = \frac{K_1 + K_3}{K_3}$$

$$R = \frac{G * b}{h_2 K_1}$$

$$m = \text{mass per unit length}$$

In equation [8], layers 1 and 3 are the face layers, of thickness h_1 and h_3 respectively, and layer 2 is the viscoelastic core layer of thickness h_2 . A_i and I_i are the cross-sectional areas and bending moments of inertia of the two face layers, and b is the width of the beam.

Use of the complex stiffness by DiTaranto in the equation of motion for free vibration is not strictly consistent with the derivation of complex stiffness, which is based upon harmonic response. DiTaranto must make the assumption that the free vibration response is of the form $u_1 = u_1(x)e^{i\Omega t}$. In the presence of viscoelastic damping of the form in equation [2] this assumption is questionable.

By incorporating the complex shear modulus for the core, G_c , along with the Young's moduli for the two outer faces, E_1 and E_2 , the equation contains the stiffness of the beam's elastic faces, the stiffness of the viscoelastic core, and the damping present in the core.

The resulting derivation considers the longitudinal displacement in terms of the displacements in the two elastic face layers along their centroids, due to bending, and the strain in the core, due to shear stress.

Building on DiTaranto's derivations for viscoelastic sandwich beam, Mead and Markus (1969) published a paper outlining an equation for the forced vibration of viscoelastic sandwich beams. Mead and Markus noted that DiTaranto's sixth-order differential equation should not in fact be applied to the free vibration problem. The use of complex stiffness by DiTaranto can not be reconciled with the decaying nature of free vibration nor the differential equation form of the viscoelastic constitutive law. The equation however is applicable to beams with an applied harmonic excitations, such as that produced by rotating machinery. In their paper, they derived an equivalent formulation of DiTaranto's equation in terms of transverse displacements instead of the longitudinal displacements used by DiTaranto. The derivation was based on the same assumptions as before. However, a transverse loading is applied to the beam and

longitudinal and rotatory inertia are ignored. The solution of the Mead and Markus equation does not yield the natural frequencies and damping factors for viscoelastic sandwich beams as described by DiTaranto. Instead, the solution of the equation yields special resonant frequencies and forced modes of vibration. A closed form solution for the forced vibration problem is given only for these special loading cases at which the modes are uncoupled, in the sense that each mode of vibration is independent of all other modes.

The Mead and Markus forced vibration equation of motion is

$$m \left(\frac{\partial^2 w}{\partial t^2} \right) + p = q(x, t) \quad [9]$$

where m = mass per unit length

w = transverse displacement of the beam centroid

p = transverse load

$q(x, t)$ = time dependent transverse external load

The equation of motion is x dependent as well as time dependent therefore every value of x represents a different mode of vibration for the beam. The transverse load, p , contains the complex stiffness for the beam and is derived by Mead and Markus as

$$p = \frac{\partial S}{\partial x} \quad [10]$$

where S = sum of shear forces in all three sandwich layers

The shear forces in the two face plates are given as

$$S_1 = \frac{E_1 h_1^3}{12} \frac{\partial^3 w}{\partial x^3} \quad [11]$$

$$S_2 = \frac{E_2 h_2^3}{12} \frac{\partial^3 w}{\partial x^3} \quad [12]$$

For core the shear force is calculated by multiplying the shear stress τ by depth d

$$S_c = -\tau d \quad [13]$$

and

$$\tau = G^* \gamma \quad [14]$$

where G^* = complex shear modulus of the core

γ = shear strain in the core

and the depth (d) is an approximation which applies the shear stress of the core over the thickness of the core plus half of each face plate:

$$d = h_2 + \frac{1}{2}(h_1 + h) \quad [15]$$

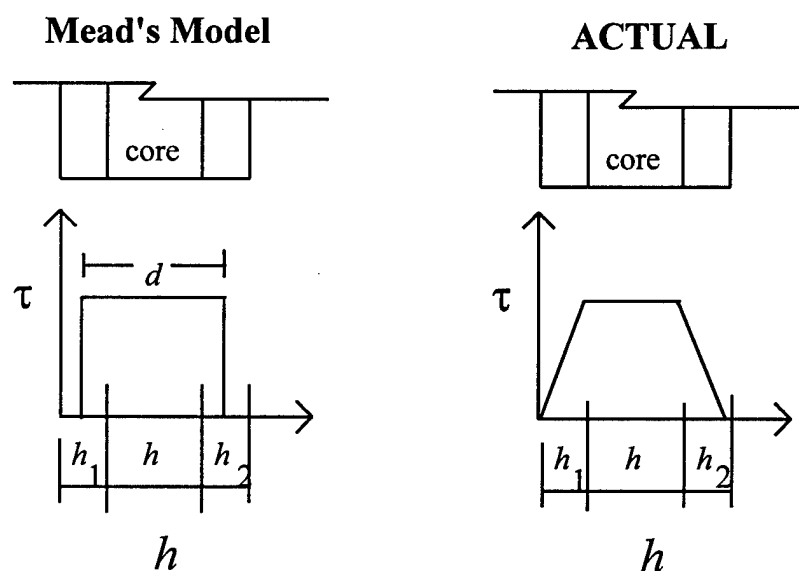
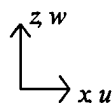


Figure 3 - Calculated depth, d , compared with

The shear strain is given as

$$\gamma = \frac{\partial w}{\partial x} + \frac{\partial u}{\partial z}$$



[16]

From the substitution of equations [10] - [16] into equation [9] and the use of the following definitions:

$$D_i = \frac{E_1 h_1^3}{12} + \frac{E_2 h_2^3}{12} \quad [17]$$

$$g = \frac{G^*}{h} \left(\frac{1}{E_1 h_1} + \frac{1}{E_2 h_2} \right) \quad [18]$$

$$Y = \frac{d^2}{D_i} \left(\frac{E_1 h_1 E_2 h_2}{E_1 h_1 + E_2 h_2} \right) \quad [19]$$

Along with the fact that the net longitudinal force in the section is zero for transverse vibration, the sixth order differential equation

$$\frac{\partial^6 w}{\partial x^6} - g(1+Y) \frac{\partial^4 w}{\partial x^4} + \frac{m}{D_i} \left(\frac{\partial^4 w}{\partial x^2 \partial t^2} - g \frac{\partial^2 w}{\partial t^2} \right) = \frac{1}{D_i} \left(\frac{\partial^2 q}{\partial x^2} - gq \right) \quad [20]$$

is derived for the forced vibratory motion of a beam.

As with DiTaranto's model, the Mead and Markus equation is limited in its practical application. To use this derivation, the special loading conditions have to be met. Although they derive the solutions to their equation for several different boundary conditions, the practical uses are also limited for any condition other than simply supported ends. For non-simply supported boundary conditions, an applied load will produce modes of vibration which may or may not be in phase with one another (Mead and Markus, 1969). That means complex values have to be used to describe these modes which greatly increase the difficulty of the problem.

Lu and Douglas (1974), compared the predicted harmonic response of the Mead and Markus model with actual sandwich beams. Through comparison of the experimental data with Mead and Markus's theoretical beam response, they were able to show that Mead and Markus's model predicted the actual behavior very well for the low frequency response, but began to lose accuracy at higher frequencies. More details of Lu and Douglas's paper will be discussed in chapter 4.

2.2 Multiple Variable Models

Although his paper deals with multi-layered plates as opposed to sandwich beams, Di Scuiiva (1987) presented a new displacement model for layered construction which offers some benefit to this discussion. Recognizing that the classic plate theory ignores the significant effect of shear deformation on thick layered plates, Di Scuiiva presented a displacement model which accounts for shear deformation in orthotropic plates. The shear deformation theory developed prior to this by Whitney and Pagano (1970) uses an arbitrary shear correction factor to correct for shear deformation of the total beam. This does not however take into account the effect of different material properties in the individual layers. In a multi-layered plate, the deformation pattern is not linear across the entire thickness of the plate, but rather it is only linear across the thickness of each layer. Di Scuiiva's model, known as the *zig-zag theory* allows for each layer to deform in a linear deformation pattern particular to that layer and still allows for displacement continuity at the interfaces. Di Scuiiva's paper points out the need to include shear deformation in multilayered material problems where some layers have a much higher modulus of elasticity others (Di Scuiiva, 1987).

Averill (1994) adapted Di Scuiiva's zig-zag model for plates to beam analysis. Averill's paper offers solutions for longitudinal, transverse, and rotational vibrations and includes the effects of shear deformation. The equations offered however do not directly deal with viscoelasticity and therefore do not consider complex stiffness. For this reason, Averill's approach did not lend itself well to the sandwich beam problem.

The paper which proved to be the most beneficial to this research was a paper published by Bai and Sun (1995). Since their model is the basis for the finite element model developed in this paper, the Bai and Sun derivation is discussed in considerable detail here. The effects of viscoelasticity on the dynamic response of sandwich beams are studied by employing a new theory which departs from the DiTaranto, Mead and Markus models. Bai and Sun eliminate the assumptions that there is perfect interface between

sandwich layers and that the top and bottom faces remain in-plane for constant transverse deformations. The core is modeled as frequency dependent viscoelastic material, while the faces are considered to be ordinary elastic beams with axial and bending resistance. There are assumptions made about the conditions at the interfaces which provide compatibility and equilibrium requirements to be satisfied which connect the behavior of the two faces together. The Bai and Sun theory also incorporates a more accurate shear deformation pattern by using a second order displacement field, Ψ , which allows the core to deform in a non-linear fashion through the thickness.

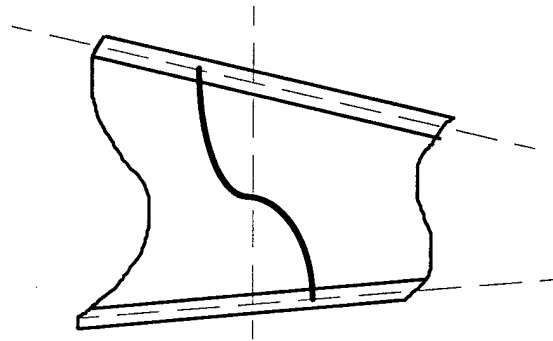


Figure 4 - Bai and Sun shear deformation, Ψ

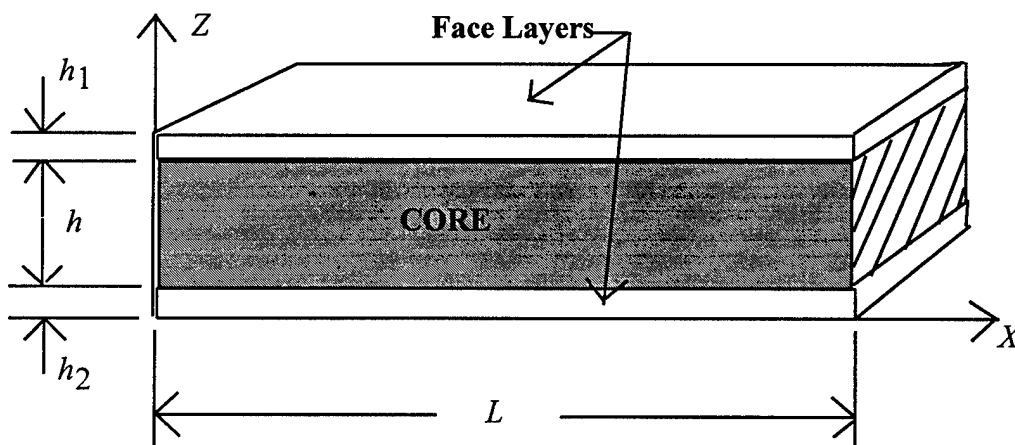


Figure 5 - Sandwich beam Construction

Also included in Bai and Sun's sandwich beam theory was the consideration of the transverse, longitudinal, and rotatory inertia all in one set of equations. The sandwich beam dimensions used by Bai and Sun are shown in Figure 5.

Displacements for the top face plates are assumed the same as for ordinary beams:

$$u'(x, z, t) = u_1(x, t) - z_1 \frac{\partial w_1(x, t)}{\partial x} \quad [21]$$

$$w'(x, z, t) = w_1(x, t) \quad [22]$$

where u' = longitudinal displacement in the top face for any (x,z) location
 u_1 = longitudinal displacement at the centroid of the top face
 z_1 = distance from centroid of top face in transverse direction
 w' = transverse displacement in the top face for any (x,z) location
 w_1 = transverse displacement at the centroid of the top face

For the bottom face plates, the displacements are taken as:

$$u^b(x, z, t) = u_2(x, t) - z_2 \frac{\partial w_2(x, t)}{\partial x} \quad [23]$$

$$w^b(x, z, t) = w_2(x, t) \quad [24]$$

where u^b = longitudinal displacement in the bottom face for any (x,z) location
 u_2 = longitudinal displacement at the centroid of the bottom face
 z_2 = distance from centroid of bottom face in transverse direction
 w^b = transverse displacement in the bottom face for any (x,z) location
 w_2 = transverse displacement at the centroid of the bottom face

Displacements for the core are assumed as follows

$$u^c(x, z, t) = u_0(x, t) + z \left(e^{\Psi(x, t)} - \frac{\partial w_0(x, t)}{\partial x} \right) - \frac{z^2}{2} \frac{\partial \Phi(x, t)}{\partial x} + \frac{z^3}{6} \frac{\partial^2 \Psi(x, t)}{\partial x^2} \quad [25]$$

$$w^c(x, z, t) = w_0(x, t) + z \Phi(x, t) - \frac{z^2}{2} \frac{\partial \Psi(x, t)}{\partial x} \quad [26]$$

where u^c = longitudinal displacement of core
 u_0 = longitudinal displacement at centroid of core
 w^c = transverse displacement of core
 w_0 = transverse displacement at centroid of core
 Ψ = shear deformation in core
 Φ = transverse normal deformation in core
 $e = 2(1 + \nu_c)$
 ν_c = Poisson's ratio for the core

In Bai and Sun's approach to the viscoelastic sandwich beam problem, an imperfect adhesive layer is assumed between the core and each of the faces. To describe the interaction at these interfaces, the adhesive layers are considered to be viscoelastic layers. A complex stiffness, k^* , is calculated for these layers and the strain energy contribution of the adhesive layers is included in the calculations for the total potential energy of the sandwich beam. This frequency dependent complex stiffness is equal to

$$k^* = k(\omega) (1 + j\delta(\omega)) \quad [27]$$

When the real portion of the adhesive layer stiffness, $k(\omega)$, is small, the adhesive layer would be soft and displacements within this layer (due to shear deformation) would therefore be possible. As $k(\omega)$ increases and approaches infinity, there would be perfect bonding between the core and the faces just as all previous sandwich beam theory has assumed.

Bai and Sun's research also suggests that since the action within these adhesive layers is viscoelastic, the adhesive layers themselves contribute to the overall damping of the sandwich beam system. One of their conclusions is that there may be an optimal adhesive layer stiffness that could be considered in achieving the maximum structural damping for the system. Because of its comparatively small thickness, the effect of adhesive layer viscoelasticity would not show up unless the adhesive layer were

significantly softer than the core itself. An adhesive layer that is stiffer than or only slightly softer than the core would not have any effect on the Bai and Sun calculations and perfect interface could be assumed. For this reason perfect interface would generally be a suitable assumption for most sandwich beams, unless adhesive layer softness were intentionally designed into the system.

Bai and Sun do reference a particular design of racing boats using sandwiched materials where soft adhesive layers increase the energy absorption of the system. However for the use of viscoelastic sandwich beams in TMDs, the effort involved in designing and constructing an adhesive layer which was soft enough to provide significant damping and sturdy enough to last over time would make it impractical. In the research present in this paper, perfect interface was assumed in all calculations. To "connect" the behavior of the two faces and the core together, there are compatibility relationships assumed at each of the core-face interfaces.

At the upper interface

$$\tau = k^*(u^f - u^c) \quad [28]$$

$$w^c = w^f \quad [29]$$

where τ = shear stress at upper interface

At the lower interface

$$\tau = k^*(u^c - u^b) \quad [30]$$

$$w^c = w^b \quad [31]$$

where τ = shear stress at lower interface

In the core

$$\tau = G_c e^{\Psi} \quad [32]$$

where τ = shear stress in core

$G_c = G^*$ = complex shear modulus for the core

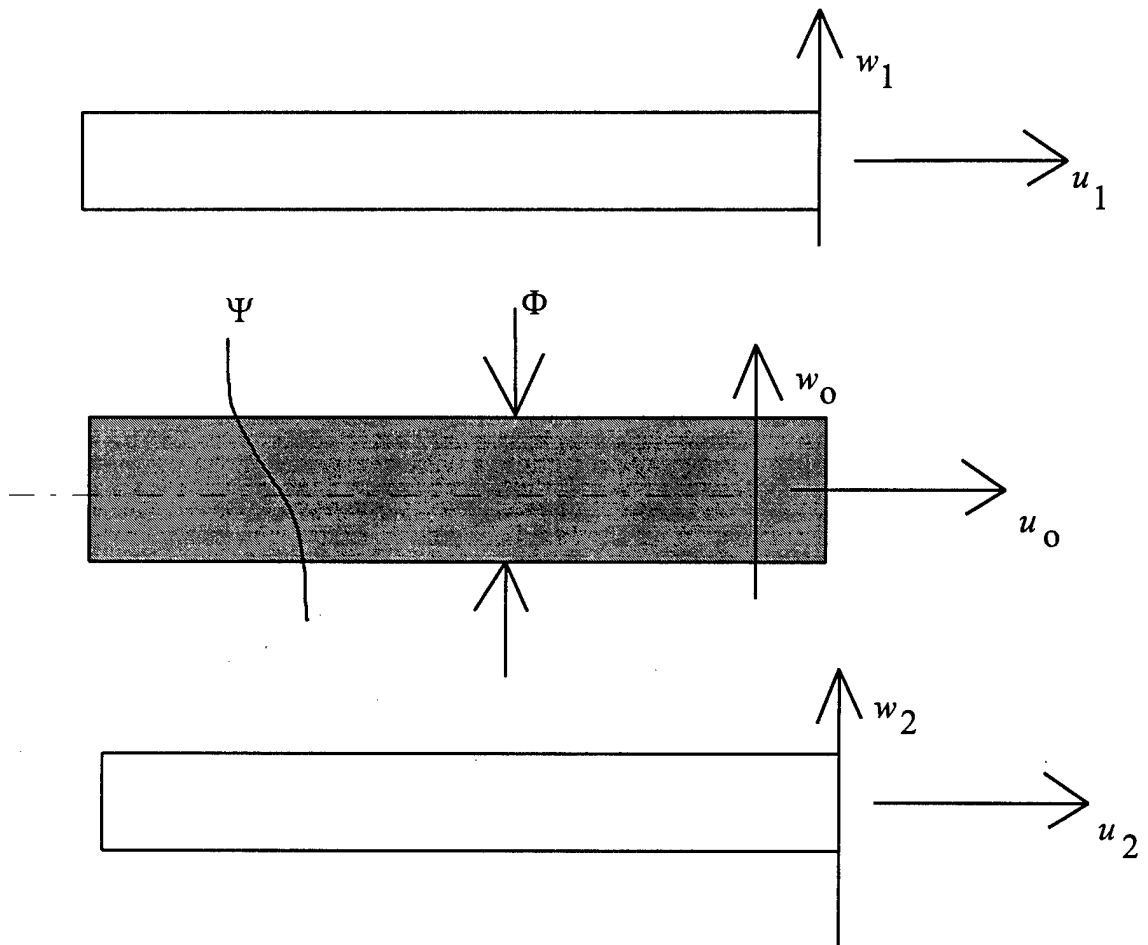


Figure 6 - Sandwich Beam Displacement Field

For equilibrium to be satisfied, the shear stress at the top interface, the shear stress in the core and the shear stress at the bottom interface must all three be equal. From this equilibrium relationship, Bai and Sun derived the equation:

$$k^* \left[u_1 - u_2 + \frac{h_1 + h}{2} \frac{\partial w_1}{\partial x} + \frac{h_2 + h}{2} \frac{\partial w_2}{\partial x} \right] - (k^* e h + 2E_c) \Psi + k^* \frac{h^3}{12} \frac{\partial^2 \Psi}{\partial x^2} = 0 \quad [33]$$

Using these compatibility equations, Bai and Sun were able to rewrite their displacement field of eight variables, into a displacement field of five variables. The details of this will be discussed later.

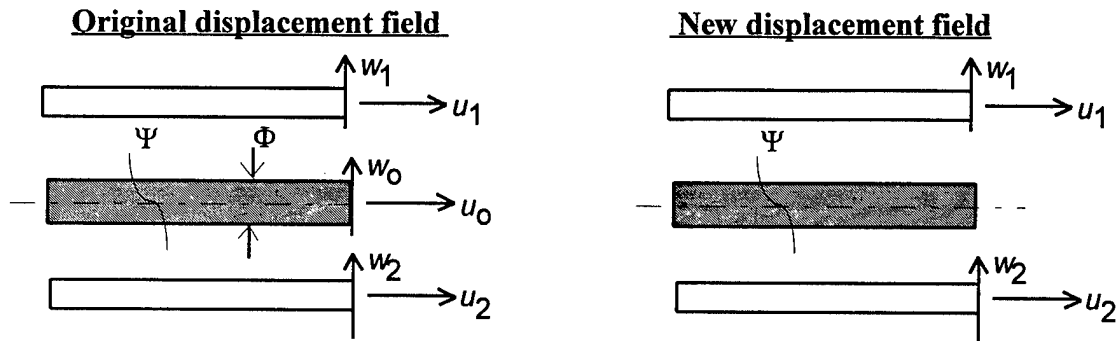


Figure 7 - Reducing Displacement Field

The governing equations of motion and the boundary conditions are derived via Hamilton's principle, which requires

$$\delta \int_{t_1}^{t_2} [T - U] dt = 0 \quad [34]$$

where T is the kinetic energy, U is the “potential energy”, and t_1 and t_2 define the time interval.

In the case of Bai and Sun's sandwich beam theory, the kinetic energy includes the longitudinal inertia of the top face, the transverse inertia of the top face, the rotatory inertia of the top face, the longitudinal inertia of the bottom face, the transverse inertia of the bottom face, the rotatory inertia of the bottom face, the longitudinal inertia of the core, and the transverse inertia of the core. The equation for the kinetic energy of the viscoelastic sandwich beam then becomes

$$T = \frac{1}{2} \int_0^L \rho_1 h_1 \left[(\dot{u}_1)^2 + \frac{h_1^2}{12} \left(\frac{\partial \dot{w}_1}{\partial x} \right)^2 + (\dot{w}_1)^2 \right] + \rho_2 h_2 \left[(\dot{u}_2)^2 + \frac{h_2^2}{12} \left(\frac{\partial \dot{w}_2}{\partial x} \right)^2 + (\dot{w}_2)^2 \right] + \int_{-h/2}^{h/2} \rho [(\dot{u}^c)^2 + (\dot{w}^c)^2] dz dx \quad [35]$$

In the case of Bai and Sun's sandwich beam theory, the potential energy includes the axial-extension stiffness of the top face, the bending stiffness of the top face, the axial-extension stiffness of the bottom face, the bending stiffness of the bottom face, the shear stiffness of the core, the transverse deformation stiffness of the core, and the shear deformation resistance of the core. It is important to note that Bai and Sun's "potential energy" calculation includes energy dissipation. The stiffness and the damping of the system are included together in one set of energy calculations through the use of complex moduli. The equation for the potential energy of the viscoelastic sandwich beam then becomes

$$U = U_1 + U_2 + U_3 + U_4 + \phi \quad [36]$$

where

$$U_1 = \frac{1}{2} \int_0^L E_1 h_1 \left[\left(\frac{\partial u_1}{\partial x} \right)^2 + \frac{h_1^2}{12} \left(\frac{\partial^2 w_1}{\partial x^2} \right)^2 \right] dx \quad [37]$$

$$U_2 = \frac{1}{2} \int_0^L E_2 h_2 \left[\left(\frac{\partial u_2}{\partial x} \right)^2 + \frac{h_2^2}{12} \left(\frac{\partial^2 w_2}{\partial x^2} \right)^2 \right] dx \quad [38]$$

$$U_3 = \frac{1}{2} \int_0^L G_c h (e\Psi)^2 dx \quad [39]$$

$$U_4 = \frac{1}{2} \int_0^L E_c h \left[\Phi^2 + \frac{h^2}{12} \left(\frac{\partial \Psi}{\partial x} \right)^2 \right] dx \quad [40]$$

To include the compatibility requirement of equation [33] for the adhesive layer, Bai and Sun used a Lagrange multiplier, λ , which represents the face-core interface shear force, and ϕ , which represents the strain energy within the adhesive layer. Thus the potential energy is augmented by the expression

$$\phi = \lambda \int_0^L \left[k * \left[u_1 - u_2 + \frac{h_1 + h}{2} \frac{\partial w_1}{\partial x} + \frac{h_2 + h}{2} \frac{\partial w_2}{\partial x} \right] - (k * eh + 2E_c) \Psi + k * \frac{h^3}{12} \frac{\partial^2 \Psi}{\partial x^2} \right] dx \quad [41]$$

By eliminating Lagrange multiplier, λ , Bai and Sun were able to translate these expressions for the potential and kinetic energy, by taking variation in the Hamilton's principle equation with respect to u_1 , u_2 , w_1 , w_2 , and Ψ . The result is a matrix of five governing equations of motion which are represented as

$$(\partial \mathbf{M}) \ddot{\mathbf{u}} + (\partial \mathbf{K}) \mathbf{u} = \mathbf{f} \quad [42]$$

where $\mathbf{u} = (u_1, w_1, u_2, w_2, \Psi)^T$
 $\partial \mathbf{M}$ = the mass matrix differential operator
 $\partial \mathbf{K}$ = the stiffness matrix differential operator
 $\mathbf{f} = (0, q, 0, 0, 0)^T$ *this is assuming an applied load, q , at the beam center*

It was also noted by Bai and Sun that $\partial \mathbf{K}$, \mathbf{u} , and $\ddot{\mathbf{u}}$ are complex. Some of the possible boundary conditions are derived by Bai and Sun for the top face, bottom face, and core of

a sandwich beam using these same Hamilton's principle derivations. However, complete solutions are not offered for all boundary conditions which could occur. There are therefore sandwich beam configurations for which analytical solutions have not been determined. Although Bai and Sun's sandwich beam theory is the basis for the analysis offered in this paper, it was necessary to use approximation techniques to develop a more inclusive sandwich beam analysis tool.

3. FINITE ELEMENT FORMULATION FOR DAMPED SANDWICH BEAMS

3.1 Prior Research

The optimal design of viscoelastic sandwich beam TMD's, requires that an analysis technique be available which could be used to find resonant frequencies and complex impedance functions for sandwich beams of any geometric and material configuration. Without an analytical solution offered by any previous research which could satisfy this requirement, the need for finite element modeling became evident.

A few researchers have developed finite element techniques to predict sandwich beam behavior. Johnson, Kienholz and Rogers (1981) developed a three-dimensional model using the MSC/NASTRAN computer program. They describe the methods available for the finite analysis of structures with viscoelastic damping as falling into three categories. The first is the complex eigenvalue method. In the formulation of this method, the free vibration response is determined using a complex stiffness matrix, which is not frequency dependent. The mass and stiffness matrices are taken as constant. A separate damping term can be added to account for viscous damping which varies with frequency. The resulting equation of motion is solved as an eigenvalue problem with complex eigenvalues and eigenvectors. There are two drawbacks to this approach. First, it is difficult to obtain realistic matrices. Very few viscoelastic materials behave in such an accommodating manner (Johnson, Kienholz, and Rogers, 1981). The second problem is computational cost. Complex eigenvalue analysis involves considerable programming and computing time.

The next method type described by Johnson, Kienholz, and Rogers is the modal strain energy method. This is the method which formed the basis of their work. By assuming that the damped sandwich beam can be represented in terms of the undamped system they were able to greatly simplify the viscoelastic sandwich beam problem. The method involves the calculation of the undamped mode shapes of the sandwich beam with the viscoelastic material treated as if it were purely elastic with a real stiffness modulus.

They then use the relationship between the viscoelastic damping factor and modal strain energy to apply modal damping to the calculations. An empirical method was also included which allows an approximate correction for the frequency dependent material properties. The modal strain energy method was also incorporated by Soni (1981) in his finite element analysis approach to viscoelastic sandwich beams. Soni used the MAGNA-D computer program for his finite element analysis. Both Johnson, Kienholz, and Rogers (1981) and Soni (1981) used 3 dimensional brick elements for their models. Johnson, Kienholz, and Rogers used an 8 node element, HEXA8, for the core layer, and a four node element, QUAD4, for the face plate layers. Soni used isoparametric elements for his model which had 8 nodes for the core layer, and 8 to 20 nodes for the face plates depending upon the face plate thickness. In both papers experimental data is presented demonstrating these two methods on simple problems with good results. However Mace (1992) criticizes these approaches as being too complex and costly to use. He points out the difficulties in creating the meshes used and the complexity of the analysis. Soni for instance used 440 active degrees of freedom for the analysis of a simple cantilever beam.

The third finite element method described by Johnson, Kienholz, and Rogers is the direct frequency response method. This is the method used in this thesis and was also used by Mace (1992). This method analyzes the harmonically forced vibration problem using complex stiffness which is frequency dependent. The system damping is accounted for in the complex nature of the stiffness. Mace directed his finite element analysis toward sandwich beams with very thin viscoelastic layers only. With the thin layer problem, he was able to assume the viscoelastic core as a film layer. The inertial effects of the viscoelastic material are considered negligible and are therefore not included in the mass matrix. The stiffness is given by two separate matrices: a stiffness matrix for the two face plates, and a frequency dependent, complex stiffness matrix for the core. At each node, Mace's model uses 5 degrees of freedom, all of which represent displacements in the two face plates. Comparing his results with experimental data and prior theoretical

studies, Mace is able to show results which are good, but only for studies involving very thin core layers. The finite element model described in this thesis is derived in much the same manner as the Mace model.

3.2 Assumptions

The finite element model derived here is based upon the assumptions made by Bai and Sun (1995). However, some of Bai and Sun's assumptions about adhesive layer behavior were discarded as unnecessary for the present study.

Bai and Sun assumed that:

1. Elastic face layers are considered to be ordinary beams with axial and bending resistance.
2. The viscoelastic core carries negligible longitudinal stress, but takes non-linear displacement fields in both x and z directions.
3. Longitudinal displacement discontinuity between the two face plates is proportional to the shear stress at the face-core interface, which is viscoelastic.
4. Shear stress at top and bottom interfaces equals the shear stress in the core layer
5. Transverse displacement of faces equals transverse displacement of core at interfaces

For the purpose of the derivations set forth in this paper, perfect adhesive layer interaction was assumed for all cases. The result is that everywhere in Bai and Sun's calculations where the adhesive layer stiffness, k^* , appears, a value of infinity can be assumed. At the interfaces, this infinitely stiff adhesive layer transmits the shear stress unchanged from the core to the face layers.

The original displacement field includes eight displacements. Using the compatibility and equilibrium equations, Bai and Sun were able to reduce this to five displacements. The following is a summary of how this was accomplished.

(a) At the upper interface, the transverse displacement, w , of the core is equal to the transverse displacement of the top face. Substituting equations [22] and [26] into equation [29] with

$$w^c\left(\frac{h}{2}\right) = w^t\left(-\frac{h_1}{2}\right)$$

yields the equation

$$w_1 = w_0 + \frac{h}{2}\Phi - \frac{h^2}{8}\frac{\partial\Psi}{\partial x} \quad [43]$$

(b) At the lower interface, the transverse displacement, w , of the core is equal the transverse displacement of the bottom face. Substituting equations [24] and [26] into equation [31] with

$$w^c\left(-\frac{h}{2}\right) = w^b\left(\frac{h_2}{2}\right)$$

yields the equation

$$w_2 = w_0 - \frac{h}{2}\Phi - \frac{h^2}{8}\frac{\partial\Psi}{\partial x} \quad [44]$$

(c) Solving equations [43] and [44] for w_0 and Φ yields

$$w_0 = \frac{w_1 + w_2}{2} + \frac{h^2}{8}\frac{\partial\Psi}{\partial x} \quad [45]$$

and

$$\Phi = \frac{w_1 - w_2}{h} \quad [46]$$

In the remainder of the discussion, a simplified partial differential equation notation will be used, to reduce the length of the equations

$$\begin{aligned} \frac{\partial(\cdot)}{\partial x} & \text{ becomes } (\cdot)_{,X} \\ \frac{\partial^2(\cdot)}{\partial x^2} & \text{ becomes } (\cdot)_{,XX} \\ \frac{\partial^3(\cdot)}{\partial x^3} & \text{ becomes } (\cdot)_{,XXX} \end{aligned}$$

Thus, for instance Equation [45] becomes

$$w_0 = \frac{w_1 + w_2}{2} + \frac{h^2}{8} \Psi_{,x}$$

(d) At the upper interface, the longitudinal displacement, u , of the core equals the longitudinal displacement of the top face. Substituting equations [21] and [25] into equation [28] with

$$u^c\left(\frac{h}{2}\right) = u'\left(-\frac{h_1}{2}\right)$$

yields the equation

$$u_1 + \frac{h_1}{2} w_{1,x} = u_0 + \frac{h}{2} (e\Psi - w_{0,x}) - \frac{h^2}{8} \Phi_{,x} + \frac{h^3}{48} \Psi_{,xx} \quad [47]$$

(e) At the lower interface, the longitudinal displacement, u , of the core equals the longitudinal displacement of the bottom face. Substituting equations [23] and [25] into equation [30] with

$$u^c\left(-\frac{h}{2}\right) = u^b\left(\frac{h_2}{2}\right)$$

yields the equation

$$u_2 - \frac{h_2}{2} w_{2,x} = u_0 - \frac{h}{2} (e\Psi - w_{0,x}) - \frac{h^2}{8} \Phi_{,x} - \frac{h^3}{48} \Psi_{,xx} \quad [48]$$

(f) Solving equations [47] and [48] allows u_0 to be expressed in terms of the face plate displacements only as

$$u_0 = \frac{1}{2} \left[u_1 + u_2 + \left(\frac{h_1}{2} + \frac{h}{4} \right) w_{1,x} - \left(\frac{h_2}{2} + \frac{h}{4} \right) w_{2,x} \right] \quad [49]$$

The displacement field of eight variables can now be represented by five variables. To reduce the size of the problem even further the last compatibility expression, equation [33] is used. When the adhesive layer stiffness, k^* , is taken to be infinite, this expression can be re-written as

$$\Psi_{,xx} - \frac{12e}{h^2} \Psi = \frac{12}{h^3} \left[u_2 - u_1 - \left(\frac{h_1 + h}{2} \right) w_{1,x} - \left(\frac{h_2 + h}{2} \right) w_{2,x} \right] \quad [50]$$

Using this expression, it is possible to eliminate from the displacement field the variable Ψ . Initial attempts to include Ψ as a variable in the finite element formulation were unsuccessful, resulting in badly behaved finite element models. However, insight was gained from those initial attempts that permitted an approximate model to be constructed successfully.

The first attempted element derivation simply replaced $\Psi_{,xx}$ in the variational formulation with the expression

$$\Psi_{,xx} = \frac{12e}{h^2} \Psi + \frac{12}{h^3} \left[u_2 - u_1 - \left(\frac{h_1 + h}{2} \right) w_{1,x} - \left(\frac{h_2 + h}{2} \right) w_{2,x} \right] \quad [51]$$

Then Ψ was approximated using linear shape functions as

$$\Psi(x,t) = \left(1 - \frac{x}{L}\right)\Psi_i + \frac{x}{L}\Psi_j \quad [52]$$

within the element. This approximation led to a badly behaved element whose stiffness appeared to increase as the number of elements were increased.

A second attempt to include Ψ explicitly as a nodal variable was likewise unsuccessful, but suggested the final form of the model. Equation [50] is a differential equation for $\Psi(x,t)$ in terms of the face plate displacements and their derivatives. Assuming harmonic response of u_1, u_2, w_1, w_2 , and Ψ allows equation [50] to be rewritten as an ordinary differential equation describing the spatial variation of Ψ at any given time, t . The solution of this differential equation is given as the sum of the homogeneous solution Ψ_h and the particular solution Ψ_p .

Taken as an ordinary differential equation, equation [50] is quite easy to handle, as the coefficients are constant. The homogeneous solution is of the form

$$\Psi_h(x) = \alpha_1 e^{\sqrt{\frac{12e}{h^2}}x} + \alpha_2 e^{-\sqrt{\frac{12e}{h^2}}x} \quad [53]$$

which can also be written as

$$\Psi_h(x) = A_1 \cosh\sqrt{\frac{12e}{h^2}}x + A_2 \sinh\sqrt{\frac{12e}{h^2}}x \quad [54]$$

The homogeneous solution can be used to construct a particular solution, by the method of variation of parameters, for given u_1, u_2, w_1 , and w_2 functions. However a more straight forward approach is to recognize that the homogeneous solution contains all

information needed to construct the nodal equations, since it contains the boundary information. Thus, it was decided to construct a new set of shape functions for $\Psi_h(x)$ using the homogeneous solution of equation [54]. This leads to the new equations

$$\Psi(x,t) = \frac{\sinh\left[\sqrt{\frac{12e}{h^2}}(L-x)\right]}{\sinh\left[\sqrt{\frac{12e}{h^2}}(L)\right]}\Psi_i(t) + \frac{\sinh\left[\sqrt{\frac{12e}{h^2}}(x)\right]}{\sinh\left[\sqrt{\frac{12e}{h^2}}(L)\right]}\Psi_j(t) \quad [55]$$

This shape function for $\Psi(x,t)$ also proved to be unsatisfactory, and in fact led to singular equations. Investigation into the variation of the shape functions of equation [55] revealed that the influence of boundary conditions upon the function $\Psi(x,t)$ extends only a very short distance into the beam for most realistic values of $\frac{h}{L}$. Figure 8 illustrates this point. On this figure, the value of the left hand shape function as a function of $\frac{h}{L}$ is plotted for various values of $\frac{h}{L}$. It is seen from this figure that the shape function effectively reaches zero for $\frac{h}{L} < 0.1$ and $\frac{x}{L} > \text{about } 0.1$. Thus for the relatively thin sandwiches likely to be used in the development of a viscoelastically damped sandwich beams, boundary conditions do not propagate very far into the beam. Similarly, any local variation of Ψ within the beam should not propagate. This suggests that the second derivative term in equation [50] is of minor importance, and we may approximately state

$$\Psi(x) \approx \frac{1}{eh} \left[u_2 - u_1 - \left(\frac{h_1 + h}{2} \right) w_{1,x} - \left(\frac{h_2 + h}{2} \right) w_{2,x} \right] \quad [56]$$

This approximation should be satisfactory provided the ratio $\frac{h}{L}$ is sufficiently small.

As the beam is subdivided into small beam elements the ratio of core thickness to beam element length, $\frac{h}{L}$, increases which suggests the number of elements that can effectively

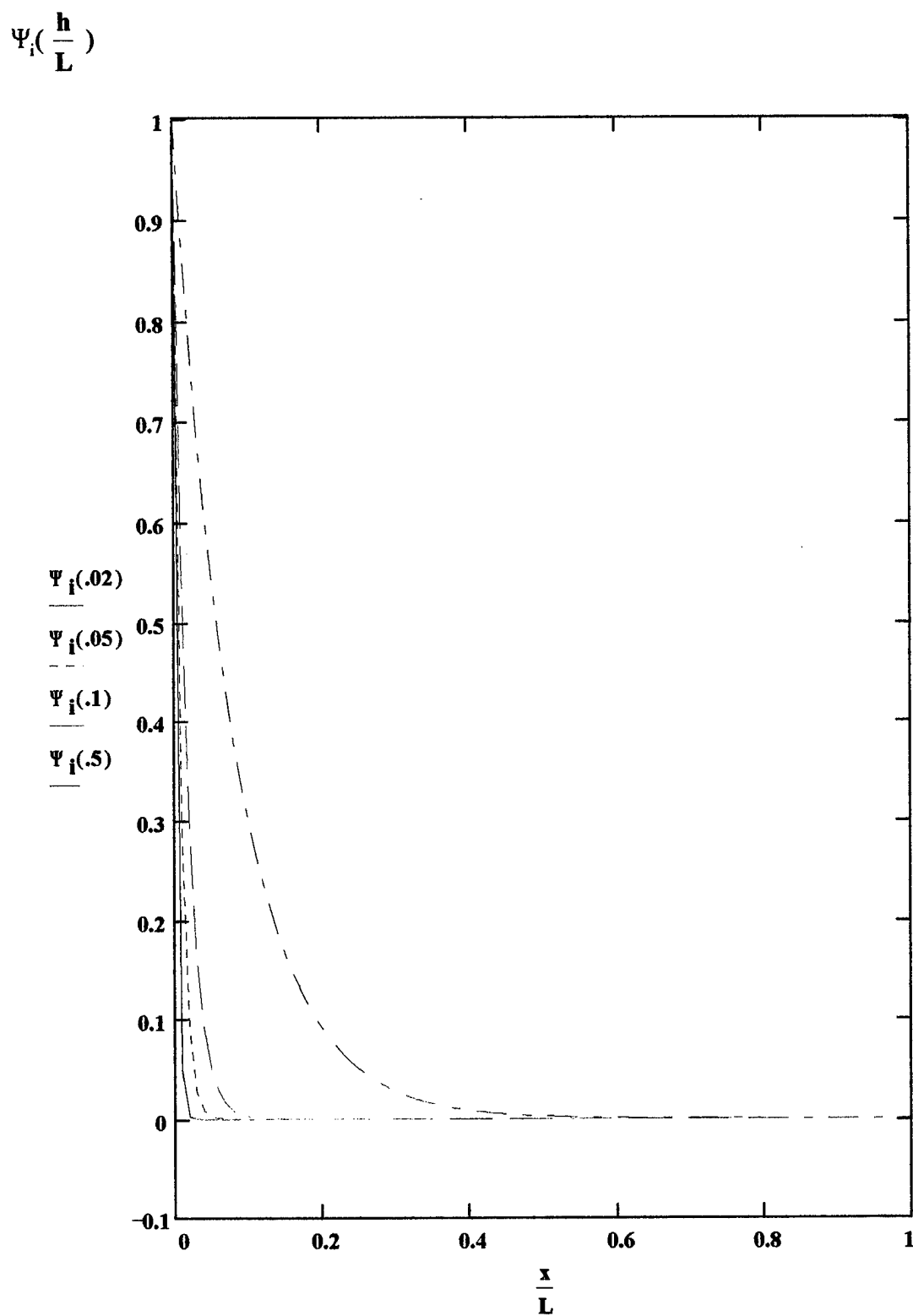


Figure 8 - Plot showing effect of core thickness on shear deformation, Ψ

be used for a given beam, before this assumption becomes invalid, has a limit. For example, if a beam of length 50 inches has a core thickness of .5 inches, the ratio $\frac{h}{L}$ is .01 which is small. If during the finite element process the beam were discretized into 50 elements, the ratio $\frac{h}{L}$ would go up to .5 for each of these beam elements. This suggests that the homogeneous portion of the shear deformation would become important for the entire length of the beam element. Thus, two important questions to be addressed in the analysis is whether sufficiently accurate frequency response information can be obtained without resorting to this level of discretization, and whether the approximation does in fact cause the element to perform badly for fine discretization meshes.

With the approximation introduced by equation [56] it is possible to eliminate Ψ from the model. The displacement field is now expressed in terms of four displacements: the transverse and longitudinal displacements of the top face plate (u_1 and w_1) and the transverse and longitudinal displacements of the bottom face plate (u_2 and w_2). Since the compatibility equation [33] has been explicitly accounted for, it is further possible to eliminate the term ϕ from the total potential energy.

3.3 Assuming Shape Functions

In their equations for potential and kinetic energy, Bai and Sun define the energy equations in terms of the displacements and the partial derivatives of the displacements with respect to x . Because these displacements are both functions of x and t , the solution of these equations requires that these displacements be separated into two distinct displacements- one a function of x and one a function of t .

In general the separation of variables takes the form

$$u_1(x,t) = \alpha_1(x)u_1(t) \quad [57]$$

$$w_1(x,t) = \beta_1(x)w_1(t) \quad [58]$$

$$u_2(x, t) = \alpha_2(x)u_2(t) \quad [59]$$

$$w_2(x, t) = \beta_2(x)w_2(t) \quad [60]$$

In the case of the model developed for harmonic response, these equations can be reduced to the form

$$u_1(x, t) = \alpha_1(x)e^{\omega_j t} \quad [61]$$

$$w_1(x, t) = \beta_1(x)e^{\omega_j t} \quad [62]$$

$$u_2(x, t) = \alpha_2(x)e^{\omega_j t} \quad [63]$$

$$w_2(x, t) = \beta_2(x)e^{\omega_j t} \quad [64]$$

It is thus possible to solve the energy equations as functions of x , for a given ω . Once the functions $\alpha_1(x)$, $\beta_1(x)$, $\alpha_2(x)$, and $\beta_2(x)$ are specified in terms of shape functions and nodal values this solution yields the mass and stiffness matrices for the sandwich beam system. The shape functions are chosen in the usual manner.

In the Bai and Sun potential and kinetic energy equations, the displacements are defined in terms of partial derivatives of the displacements. The displacement field has been reduced to four variables. The two longitudinal displacements, u , show up in the energy equation as first order derivatives. The shape functions chosen to represent them are the standard C_0 shape functions used for truss elements and are shown in Figure 9.

The two transverse displacements, w , used in this derivation show up in the energy equation as second order derivatives. The shape functions chosen to represent them are the standard beam shape functions, shown in Figure 10. Third order derivatives for the

1st Order Shape Functions

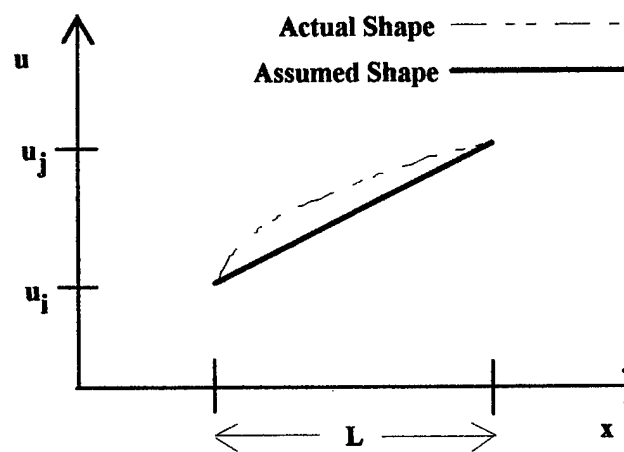
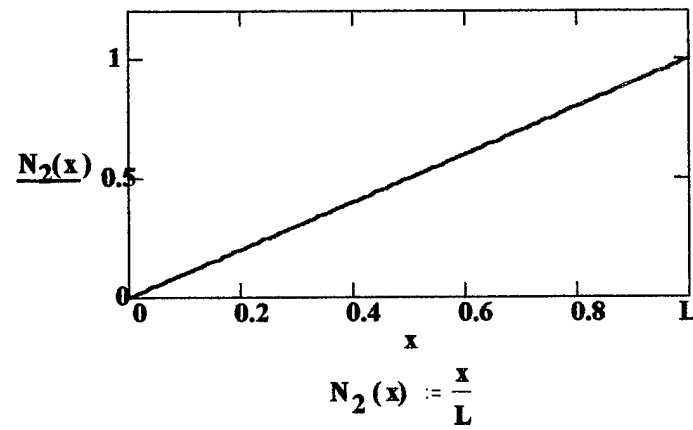
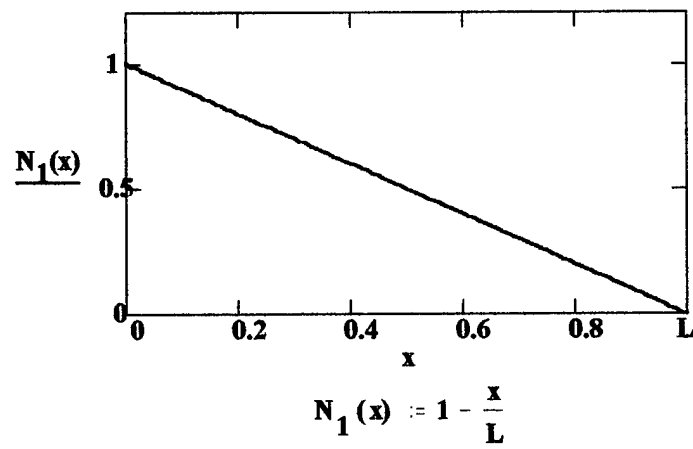
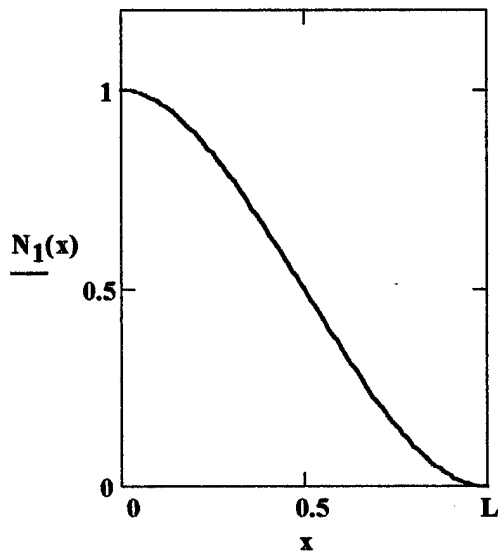
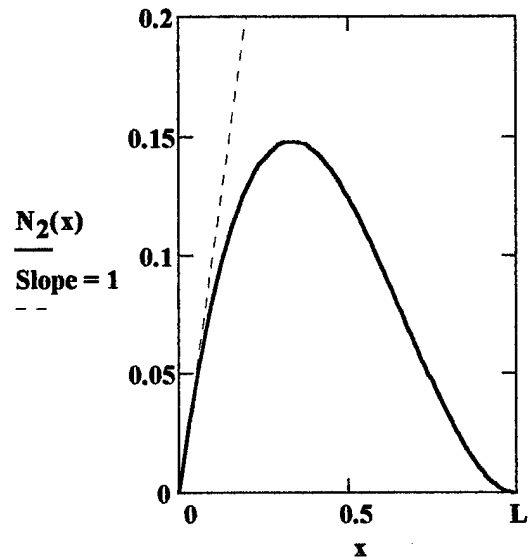


Figure 9 - 1st Order Beam Shape Functions

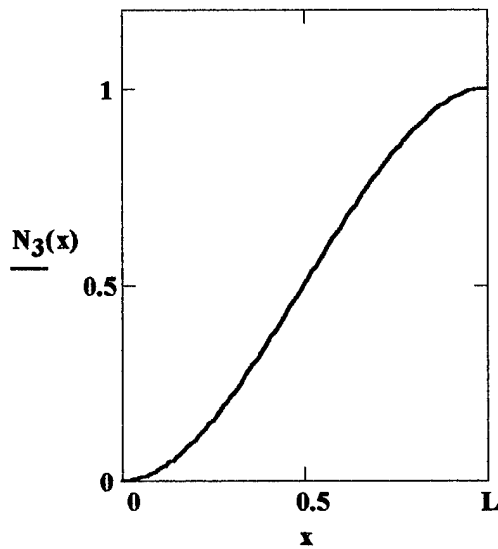
SHAPE FUNCTIONS



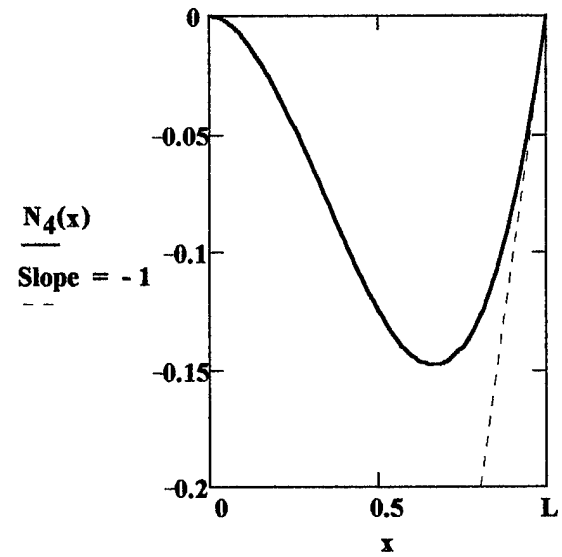
$$N_1(x) := 1 - 3 \cdot \left(\frac{x}{L}\right)^2 + 2 \cdot \left(\frac{x}{L}\right)^3$$



$$N_2(x) := L \cdot \left[\left(\frac{x}{L}\right) - 2 \cdot \left(\frac{x}{L}\right)^2 + \left(\frac{x}{L}\right)^3 \right]$$



$$N_3(x) := 3 \cdot \left(\frac{x}{L}\right)^2 - 2 \cdot \left(\frac{x}{L}\right)^3$$



$$N_4(x) := L \cdot \left[-\left(\frac{x}{L}\right)^2 + \left(\frac{x}{L}\right)^3 \right]$$

Figure 10 - 2nd Order Beam Shape Functions

transverse displacements appear in the kinetic energy equations once all substitutions have been made. This however shows up only as part of the term for the longitudinal inertia of the core. Since the core density is usually significantly smaller than the face density, this inertia term is small. The third derivative terms therefore have little effect on the behavior of the beam system and were not considered when determining shape functions.

When the interpolation functions are placed into the energy equations, it is then possible to carry-out the integration of the energy equations and form the mass and stiffness matrices. With the inclusion of the interpolation functions, the displacement field becomes a vector of six displacements at each beam node.

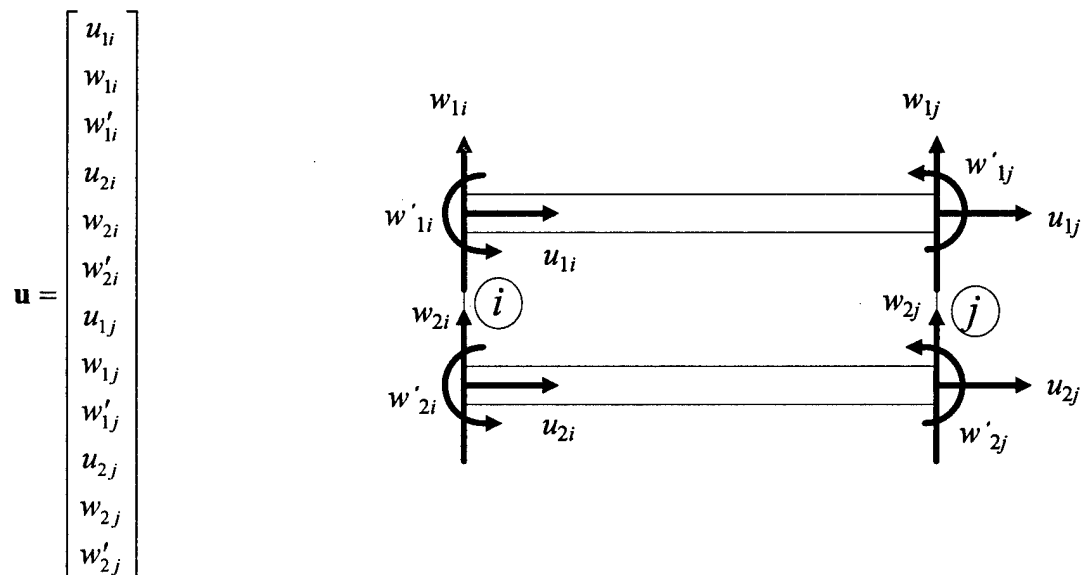


Figure 11 - Displacement Vector

With twelve displacements to be calculated, the element mass and stiffness matrices become twelve by twelve matrices. It is impractical to include all the details of the mass and stiffness matrix formulations in this thesis since the work involved in assembling

these twelve by twelve matrices is long and tedious. It should be noted that since the top and bottom face plates are taken to behave as ordinary elastic beams, portions of these matrices correspond to standard beam matrices where the displacements (u , w , and w') are considered. The complete matrices are provided in Appendix 1. The assembled matrices are also included as part of the FORTRAN program located in Appendix 2.

Because of the uniqueness of the viscoelastic sandwich beam system, pre-developed finite element codes typically do not address the structural analysis of such systems. To perform the discretization and assembly process of the finite element method, it was therefore necessary to write a computer program especially for the sandwich beam problem. This was accomplished using the FORTRAN programming language.

3.4 FORTRAN Program

The FORTRAN program was written with the mass and stiffness matrices included in the programming. These matrices are provided with unknown variables allowing the program to model any sandwich beam configuration. No attempt was made at this stage of element development to develop a general code, but the element developed should be easily incorporated into such a program.

Once the sandwich beam information is provided, the mass and stiffness matrices for each element are calculated and stored. The program then must assemble each of the individual element matrices into one a global mass and stiffness matrix for the entire beam. By defining the displacement field so that the displacements for each end node are kept together, it was possible to add these matrices in a convenient manner. The displacements for node j for one element are the same as the displacements for node i for the next element and so forth.

3.5 Equation of Motion

Once mass and stiffness matrices were derived, the equation of motion could be determined. Using the direct frequency response method the form of the equation of motion for a beam element will be

$$\mathbf{M}\ddot{\mathbf{u}} + \mathbf{K}^*\mathbf{u} = \mathbf{q}(t) \quad [65]$$

where \mathbf{M} = mass matrix

\mathbf{u} = nodal displacement vector

$\ddot{\mathbf{u}}$ = nodal acceleration vector

\mathbf{K}^* = complex stiffness matrix, dependent upon Ω

$\mathbf{q}(t)$ = nodal force vector

If a harmonic load is applied

$$\mathbf{q}(t) = \mathbf{Q}e^{i\Omega t} \quad [66]$$

where Ω is the forcing frequency. Both amplitude and mode of vibration are dependent on the frequency. It can be assumed that the response due to this applied harmonic load will also be harmonic and at the same frequency, Ω . Then

$$\mathbf{u} = \mathbf{U} e^{i\Omega t} \quad [67]$$

$$\ddot{\mathbf{u}} = -\Omega^2 \mathbf{U} e^{i\Omega t} \quad [68]$$

The equation of motion then becomes

$$(\mathbf{K}^* - \Omega^2 \mathbf{M}) \mathbf{U} = \mathbf{F}_0 \quad [69]$$

where $\mathbf{U} = (u_{1i}, w_{1i}, w'_{1i}, u_{2i}, w_{2i}, w'_{2i}, u_{1j}, w_{1j}, w'_{1j}, u_{2j}, w_{2j}, w'_{2j})^T$

\mathbf{M} = the mass matrix

\mathbf{K}^* = the stiffness matrix

$\mathbf{F}_0 = (0, \mathbf{Q}, 0, 0, 0, 0, 0, 0, 0, 0, 0, 0)^T$

This equation of motion then describes the response of the sandwich beam with an applied harmonic load and likewise the response of one beam element.

The FORTRAN program, uses an iterative process to combine the mass and stiffness matrices over a range of forcing frequencies. Because the stiffness matrix is frequency dependent, the matrix must be recalculated for each new frequency.

3.6 FORTRAN Solution Process

Using inputted information about a sandwich beam's geometry and material properties, the FORTRAN program is able to solve the sandwich beam problem. The first step in this solution process is to calculate the mass matrix. The mass matrix, \mathbf{M} , is not frequency dependent and therefore constant. Next the program begins an iterative

process for each frequency to be considered. For a given frequency, Ω , the core properties are calculated using the appropriate material-frequency function. Using these core properties, the complex stiffness matrix, \mathbf{K}^* , is updated. The matrix $\mathbf{K}^* - \Omega^2 \mathbf{M}$ is calculated. Using the IMSL subroutine LINCG to invert the matrix, equation [69] is solved for the nodal displacements at that frequency.

4. NUMERICAL STUDIES

To test the validity of results from the FORTRAN program, the system was used to analyze two previously investigated sandwich beam problems and results were compared. Also, by using Ansys, a computer structural analysis program, a simplified model was constructed of a sandwich beam in which the complex nature of the core was ignored. Ansys, which is also a finite element based approach, was able to determine the frequencies of the first five modes of free vibration. Results were then compared by using the FORTRAN program to find the undamped vibration response for the same beam.

4.1 Test Cases

The test cases were provided in a paper written by Lu and Douglas (1974). The purpose of their paper was to compare Mead and Markus's sandwich beam analysis to actual test cases. Bai and Sun (1995) then used the results found by Lu and Douglas to compare their model to both Mead and Markus's model and actual test data. The Mead and Markus analysis provided very accurate results for comparisons on a thin core layered sandwich beam. For comparisons on a thick core layered beam their results were again accurate for the first and second modes of vibration. After that the results began to skew from the actual test data and became worse as each higher mode was reached. Bai and Sun's model however remained consistently accurate even at the higher modes of excitation. The two test cases were based on a sandwich beam with the characteristics as shown in Table 1. The core material used in specimen 1 was an acrylic based material which had a mass density of .000103 lb-sec²/in⁴. The frequency dependent core complex shear modulus was calculated at a temperature of 124° F to be

$$G^* = G' + jG'' \quad [70]$$

where $G' = 0.579 \ln f + 1.136 \text{ lbf/in}^2$

$G'' = 0.601 \ln f + 1.144 \text{ lbf/in}^2$

$f = \text{frequency in a range of 50 to 3000 Hz}$

The core material used in specimen 2 was neoprene with a mass density of .000115 lb-sec²/in⁴. The frequency dependent core complex shear modulus was calculated at a temperature of 77° F to be

$$G^* = G(1 + j\delta) \quad [71]$$

where $G = 0.026 \ln f + 4.754 \text{ lbf/in}^2$
 $\delta = 0.170 \ln f + 2.705 \text{ lbf/in}^2$
 $f =$ frequency in a range of 50 to 10000 Hz

The analysis was done over a range of frequencies for an applied load located at the beam center. To show results, this range of frequencies was plotted against the resulting driving point mechanical impedance of the sandwich beam system. *Mechanical impedance* is defined as the force of the applied loading over the velocity of the system in the direction of the load. For the calculation of impedance for the test cases the force is given as a vector with only one non-zero corresponding to a concentrated nodal forcing of unit magnitude.

	<u>Specimen 1</u>	<u>Specimen 2</u>
face material:	Steel	Steel
core material:	Acrylic base	Neoprene
core thickness:	.004 inches	.25 inches
top face thickness:	.25 inches	.25 inches
bottom face thickness:	.25 inches	.25 inches
beam width:	1.0 inches	2.0 inches
beam length:	24.1875 inches	18.125 inches
boundary conditions:	free-free ends	free-free ends

Table 1 - Test Case Characteristics

Using the given equation of motion from equation [69], the mechanical impedance at degree of freedom i under forcing corresponding to degree of freedom k can be defined as

$$\text{Imp}_{ik} = \frac{1}{j\Omega U_i} \quad [72]$$

The amplitude of this impedance is

$$|\text{Imp}_{ik}| = \frac{1}{\Omega \sqrt{U_i \overline{U_i}}} \quad [73]$$

where $\overline{U_i}$ = complex conjugate of U_i

Using the FORTRAN program to analyze the sandwich beam described above the mechanical impedance was calculated at several different levels of beam discretization. Plotted in Figures 12 and 14 are the results. Figure 13 shows Lu and Douglas's comparison of experimental results with Mead and Markus's analysis.

The specimen 1 sandwich beam had a very thin core of viscoelastic material. Since Bai and Sun were primarily interested in thick layer sandwich beams, they did not use this data to compare their model. Analysis of the beam by the FORTRAN program was done using an 8 element model (taking advantage of beam symmetry the beam was only modeled to the midpoint for all meshes discussed here). Results are plotted in Figure 12 where the red line represents the theoretical results and the boxes show the experimentally obtained data. The results show the FORTRAN model has a great deal of accuracy in matching the experimentally obtained data, especially at the lower frequencies.

The specimen 2 sandwich beam had a thick core of a very soft viscoelastic material. The results of Lu and Douglas's experiments with specimen 2 are plotted in Figure 13. This plot, showing the comparison of the experimentally obtained data and Mead and Markus's theory based results, demonstrates how Mead and Markus's model begins to skew at higher frequencies. Analysis of the beam was performed by the FORTRAN model and the results plotted in Figure 14 for a 2 element mesh (represented as a blue line) and an 8 element mesh (represented as a red line). The analysis provided accurate

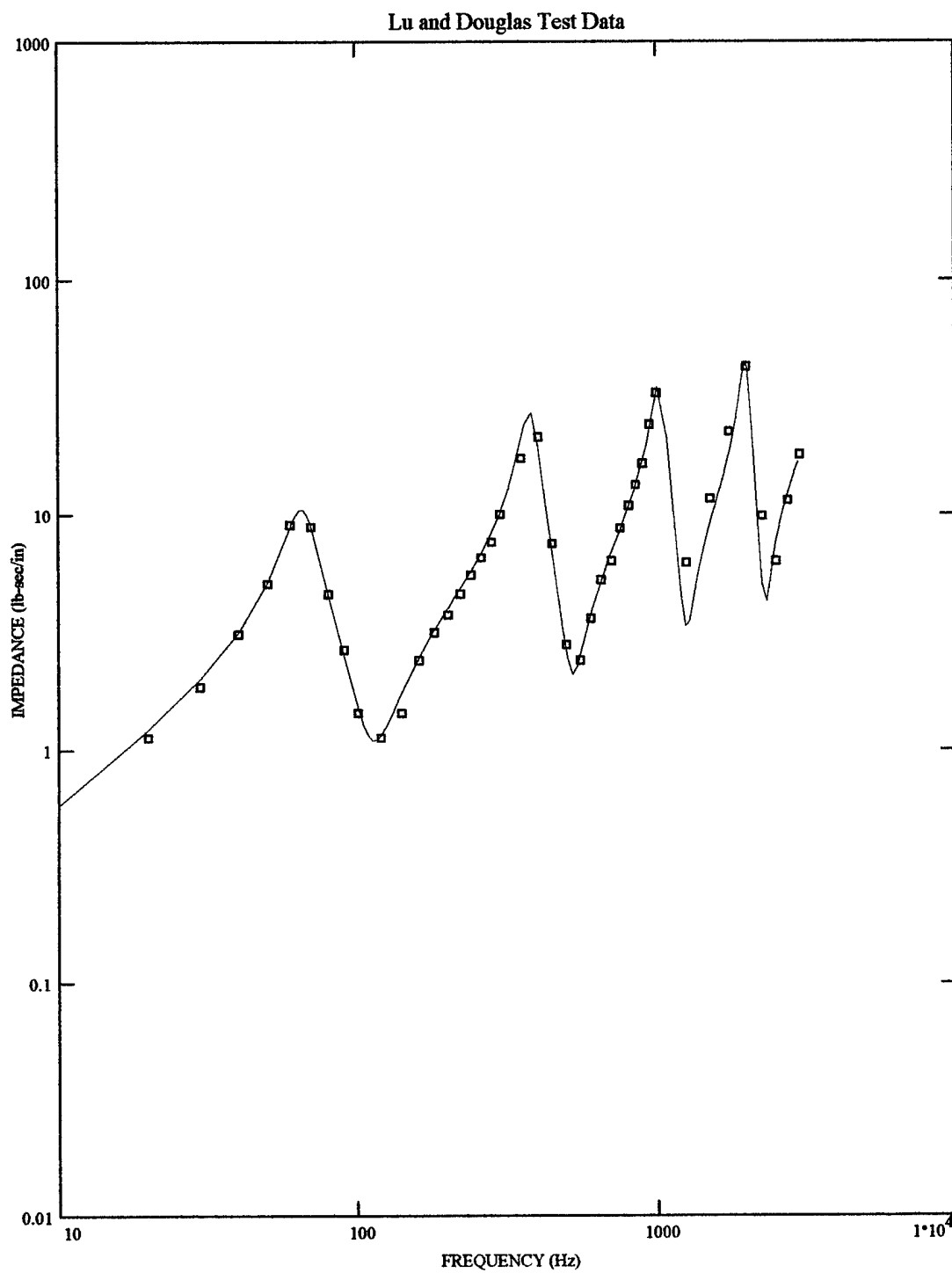


Figure 12 - Specimen 1 Test Data

Line - 8 element mesh
Boxes - Experimental Data

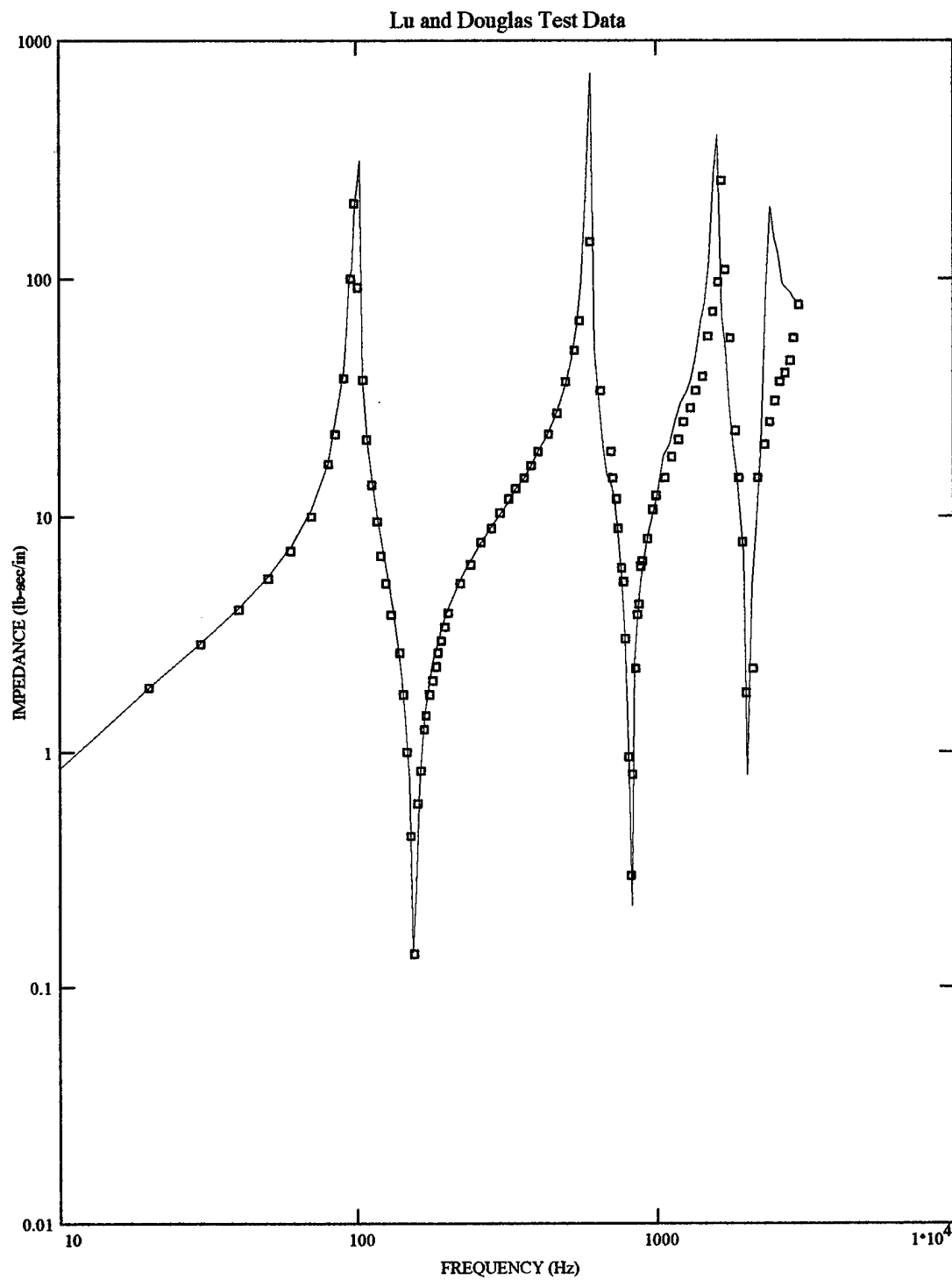


Figure 13 - Lu and Douglas Test Data

Line - Mead and Markus
Boxes - Experimental Data

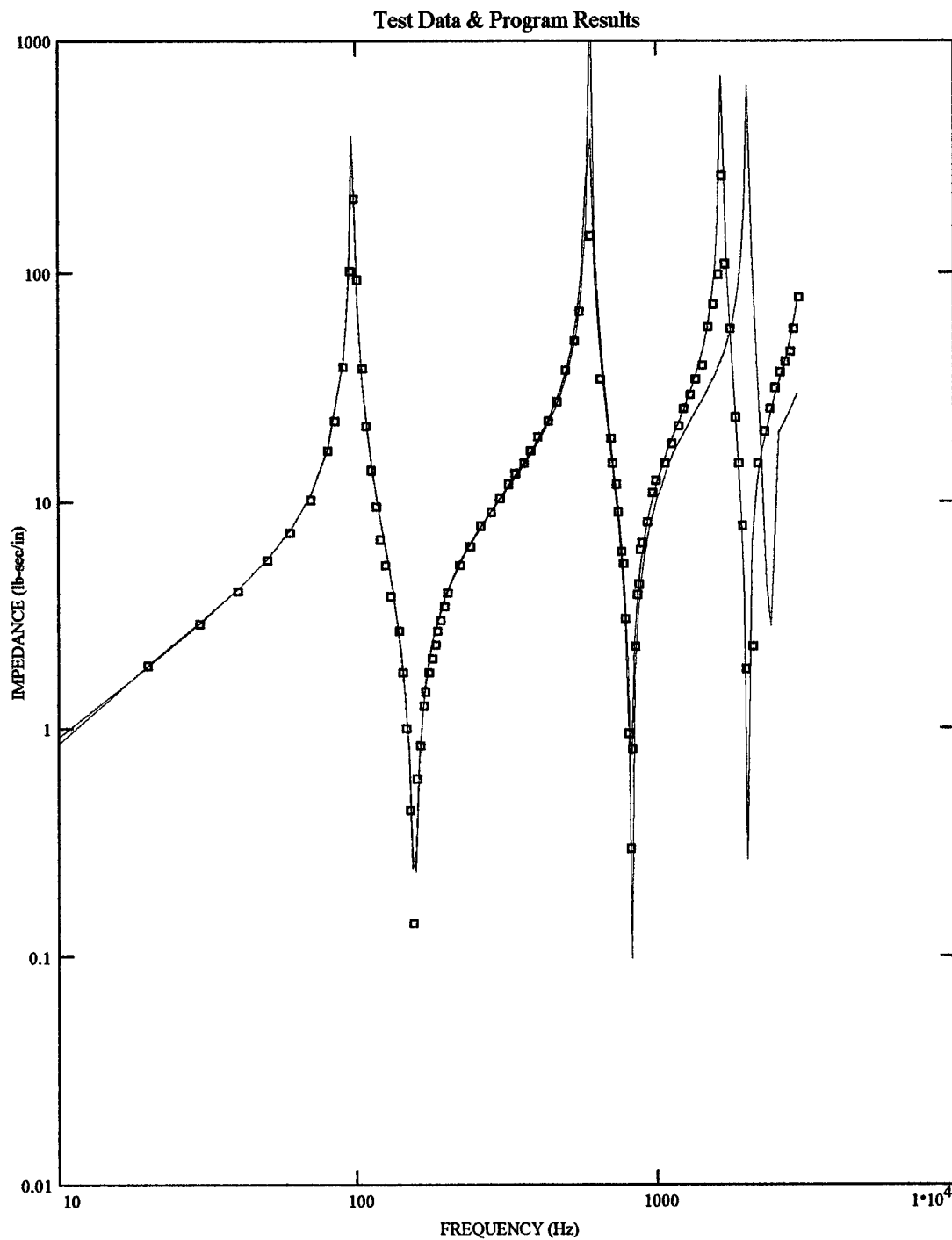


Figure 14 - Specimen 2 Test Data

Blue Line - 2 element mesh
Red Line - 8 element mesh
Boxes - Experimental Data

results for lower frequency response, even with the very crude 2 element model. As the number of elements were increased, the model began to demonstrate accuracy even at the higher frequencies. In fact, within the range of frequencies plotted, a 4 element model provided results that were very close to the 8 element results.

For additional results, an Ansys computer model was generated using the program in Appendix 3. This is a model of a beam similar to specimen 2 in geometry, however, in this analysis the damping factor was considered to be zero. In addition, the frequency dependence of the real part to the core moduli was ignored. The core stiffness was calculated as a constant equal to the specimen 2 core stiffness at a frequency of zero. The beam mesh used is shown in Figure 15. Ansys, considering the beam as a simply supported undamped system, calculated the first five modes of free vibration. As a comparison to these results, the FORTRAN model was used to analyze a similar beam problem. The damping factor was set to zero as with the Ansys model, however the frequency dependence of the real portion to the core stiffness remained. Analysis of this beam was performed as a harmonically loaded, simply supported beam. Although the differences in the analysis does not allow for an exact comparison of the Ansys and FORTRAN program results, a rough comparison demonstrates that the FORTRAN program provided modes of vibration which are analogous to the Ansys results. These results are included in Table 2.

MODE	ANSYS MODEL FREQUENCY (Hz)	FORTRAN MODEL FREQUENCY(Hz)
1	65.75981	66
2	418.15008	408
3	702.48751	667
4	765.98113	759
5	994.21499	983

Table 2 - Ansys results

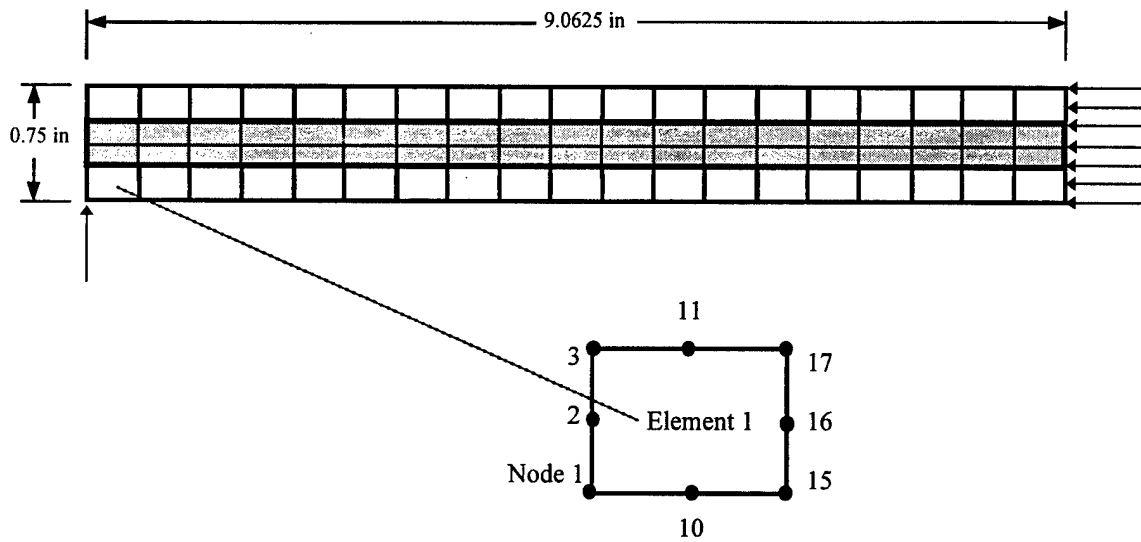


Figure 15 - Ansys model

5. CONCLUSIONS

The theoretical studies provided have shown that the finite element model developed and described in this thesis appears to be an effective analysis tool. Both thin and thick layer beams were analyzed with equally promising results. Although data was not available to compare with this model's higher frequency results (only data for frequencies up to 3000 Hz were available), the results that are available show a definite pattern of convergence towards accurate results. The use of this model for lower frequency analysis, which would constitute its predominant use, has been shown to provide good results.

Because of the assumptions about shear deformation behavior, it was assumed that it is necessary to limit the number of elements used in any mesh, so that the core thickness to beam length ratio does not become large. The theoretical studies provided encouraging information about this assumption as well. The model appears to converge very quickly for even crude meshes. This is important since it indicates that the use of this program may never require a large number of elements to achieve accurate results. Also important is that as the number of elements is increased, the results continue to converge towards accuracy. A point was never reached at which the number of elements in the mesh began to diverge away from the correct results. This indicates that even at higher core thickness to beam length ratios, the assumed shear deformation may provide good results. Further investigation would need to be performed to find if there were a limit at which the model's assumptions became invalid making the model unsuitable. With results converging as quickly as they do, a large number of beam elements would appear only to be necessary in very rare instances such as the analysis of very high frequency responses.

Although a more in-depth study of this model will be necessary before its benefits are truly known, the future application of this model is favorable. The FORTRAN model provided can be used as the basis for building future programs designed to perform many

types of analysis. The use of this model should be particularly important to the development of viscoelastic sandwich beams for use as tuned mass dampers.

Bibliography:

Auerbach, P.J. (1995) Thesis in TCC 402 at the University of Virginia. Development of a Beam-Type Tuned Mass Damper to Reduce Industrial Floor Vibration

Averill, R.C. (1994) *Composites Engineering* 4, No. 4, 381-395. Static and dynamic response of moderately thick laminated beams with damage

Bai, J.M. and Sun, C.T. (1995) *Mech. Struct. & Mach.* 23(1), 1-16. The effect of Viscoelastic Adhesive Layers on Structural Damping of Sandwich Beams

Di Scuiiva, M. (1987) *Journal of Sound and Vibration* 54, 425-442. Bending, vibration and buckling of simply supported thick multilayered orthotropic plates

DiTaranto, R.A. (1965) *Journal of Applied Mech.* 87, 881-886. Theory of the vibratory bending for elastic and viscoelastic layered finite length beams

Humar J.L. (1990) *Dynamics of Structures*. Englewood Cliffs, New Jersey: Prentice Hall

Johnson, C.D., Kienholz, D.A., and Rogers, L.C. (1981) *Shock and Vibration Bulletin* 51(1), 71-81. Finite element prediction of damping in beams with constrained viscoelastic layers

Lu, Y.P. and Douglas, B.E. (1974) *Journal of Sound and Vibration* 32, 513-516. On the forced vibrations of three layer damped sandwich beams

Mace, M. (1994) *Journal of Sound and Vibration* 172(5), 577-591. Damping of beam vibrations by means of a thin constrained viscoelastic layer: Evaluation of a new theory

Mead, D.J. and Markus, S. (1969) *Journal of Sound and Vibration* 10, 163-175. The forced vibration of a three-layer, damped sandwich beam with arbitrary boundary conditions

Plantema, F.J. (1966) *Sandwich Construction, the Bending and Buckling of Sandwich Beams, Plates, and Shells*. New York: John Wiley and Sons, Inc.

Soni, M.L. (1981) *Shock and Vibration Bulletin* 51(1), 97-109. Finite element analysis of viscoelastically damped sandwich structures

Snowdon, J.C. (1968) *Vibration and Shock in Damped Mechanical Systems*. New York: John Wiley and Sons, Inc.

Whitney, J.M. and Pagano, N.J. (1970) *Journal of Applied Mechanics* 37, 1031-1036. Shear deformation in heterogeneous anisotropic plates

Xu, Y.L., Kwok, K.S. and Samali, B. (1992) *Journal of Wind Engineering and Industrial Aerodynamics* 40, 1-32. Control of wind-induced tall building vibration by tuned mass dampers

Zienkiewicz, O.C. and Taylor, R.L. (1989) *The Finite Element Method, Fourth Edition*. London: McGraw-Hill Book Company

APPENDIX 1
Mass and Stiffness Matrices

The complex stiffness matrix , $\mathbf{K}^* = \mathbf{K}_1 + \mathbf{K}_2 + \mathbf{K}_3 + \mathbf{K}_4$

and

the mass matrix , $\mathbf{M} = \mathbf{M}_1 + \mathbf{M}_2 + \mathbf{M}_3$

where \mathbf{K}_1 , \mathbf{K}_2 , \mathbf{K}_3 , \mathbf{K}_4 , \mathbf{M}_1 , \mathbf{M}_2 , and \mathbf{M}_3 are shown on the following pages

$$\begin{aligned}
U_{55} &= \frac{hp}{840L^3e^2}(21h^2h_1^2 + 104e^2L^4 - 42eh^2L^2 - 42ehh_1L^2 + 21h^4 + 42h^3h_1) \\
U_{56} &= \frac{hp}{5040L^2e^2}(63h^2h_1^2 + 88e^2L^4 - 126eh^2L^2 - 126ehh_1L^2 + 63h^4 + 126h^3h_1) \\
U_{57} &= \frac{-hp}{280L^3e^2}(7h^2h_1^2 - 12e^2L^4 - 14eh^2L^2 - 14ehh_1L^2 + 7h^4 + 14h^3h_1) \\
U_{58} &= \frac{hp}{5040L^2e^2}(63h^2h_1^2 - 52e^2L^4 - 21eh^2L^2 - 21ehh_1L^2 + 63h^4 + 126h^3h_1) \\
U_{66} &= \frac{hp}{2520Le^2}(21h^2h_1^2 + 8e^2L^4 - 14eh^2L^2 - 14ehh_1L^2 + 21h^4 + 42h^3h_1) \\
U_{00} &= \frac{hp}{2520Le^2}(21h^2h_2^2 + 8e^2L^4 - 14eh^2L^2 - 14ehh_2L^2 + 21h^4 + 42h^3h_2) \\
U_{10} &= \frac{-hp}{5040L^2e^2}(63h^2h_2^2 - 52e^2L^4 - 21eh^2L^2 - 21ehh_2L^2 + 63h^4 + 126h^3h_2) \\
U_{68} &= \frac{-hp}{5040Le^2}(-21h^2h_1^2 + 12e^2L^4 - 7eh^2L^2 - 7ehh_1L^2 - 21h^4 - 42h^3h_1) \\
U_{99} &= \frac{hp}{840L^3e^2}(21h^2h_2^2 + 104e^2L^4 - 42eh^2L^2 - 42ehh_2L^2 + 21h^4 + 42h^3h_2) \\
U_{90} &= \frac{hp}{5040L^2e^2}(63h^2h_2^2 + 88e^2L^4 - 126eh^2L^2 - 126ehh_2L^2 + 63h^4 + 126h^3h_2) \\
U_{91} &= \frac{-hp}{280L^3e^2}(7h^2h_2^2 - 12e^2L^4 - 14eh^2L^2 - 14ehh_2L^2 + 7h^4 + 14h^3h_2) \\
U_{11} &= \frac{hp}{5040Le^2}(21h^2h_2^2 - 12e^2L^4 + 7eh^2L^2 + 7ehh_2L^2 + 21h^4 + 42h^3h_2) \\
U_{59} &= \frac{hp}{840L^3e^2}(-42eh^2L^2 + 52e^2L^4 + 21h^2h_1h_2 + 21h^3h_1 - 21ehh_2L^2 - 21ehh_1L^2 + 21h^4 + 21h^3h_2)
\end{aligned}$$

$$U_{69} = \frac{-hp}{10080L^2e^2}(252eh^2L^2 - 88e^2L^4 - 126h^2h_1h_2 - 126h^3h_1 + 21ehh_2L^2 + 231ehh_1L^2 - 126h^4 - 126h^3h_2)$$

$$U_{79} = \frac{hp}{280L^3e^2}(14eh^2L^2 + 6e^2L^4 - 7h^2h_1h_2 - 7h^3h_1 + 7ehh_2L^2 + 7ehh_1L^2 - 7h^4 - 7h^3h_2)$$

$$U_{89} = \frac{-hp}{10080L^2e^2}(42eh^2L^2 + 52e^2L^4 - 126h^2h_1h_2 - 126h^3h_1 + 21ehh_2L^2 + 21ehh_1L^2 - 126h^4 - 126h^3h_2)$$

$$U_{50} = \frac{hp}{10080L^2e^2}(-252eh^2L^2 + 88e^2L^4 + 126h^2h_1h_2 + 126h^3h_1 - 21ehh_1L^2 - 231ehh_2L^2 + 126h^4 + 126h^3h_2)$$

$$U_{60} = \frac{-hp}{2520Le^2}(14eh^2L^2 - 4e^2L^4 - 21h^2h_1h_2 - 21h^3h_1 + 7ehh_2L^2 + 7ehh_1L^2 - 21h^4 - 21h^3h_2)$$

$$U_{80} = \frac{-hp}{10080Le^2}(14eh^2L^2 - 12e^2L^4 + 42h^2h_1h_2 + 42h^3h_1 + 7ehh_2L^2 + 7ehh_1L^2 + 42h^4 + 42h^3h_2)$$

M₂ - COLUMNS 1-4

$\frac{(W_{11}L^2 + 3W_{22} - 3W_{21}L)}{3L}$	$\frac{(L(-2W_{72} + LW_{71} - W_{51}) + 2(W_{52} - W_{61}))}{2L}$	$\frac{(12(W_{62} - W_{61}L) + W_{51}L^2)}{12L}$	$\frac{(-6W_{22} + 6W_{21}L + W_{11}L^2)}{6L}$
$\frac{(L(-2W_{72} + LW_{71} - W_{51}) + 2(W_{52} - W_{61}))}{2L}$	$\frac{(5L^2(-2W_{75} + LW_{77}) - 60W_{66} + 6W_{55}L^2)}{5L^2}$	$\frac{(-10W_{76}L^2 + W_{55}L^2 + 60W_{66})}{10L^2}$	$\frac{(L(2W_{72} - LW_{71} - W_{53}) - 2(W_{52} - W_{61}))}{2L}$
$\frac{(12(W_{62} - W_{61}L) + W_{51}L^2)}{12L}$	$\frac{(-10W_{76}L^2 + W_{55}L^2 + 60W_{66})}{10L^2}$	$\frac{(60W_{66} - 15W_{65}L + 2W_{55}L^2)}{15L}$	$\frac{(12W_{61}L - 12W_{62} + W_{53}L^2)}{12L}$
$\frac{(-6W_{22} + 6W_{21}L + W_{11}L^2)}{6L}$	$\frac{(L(2W_{72} - LW_{71} - W_{53}) - 2(W_{52} - W_{61}))}{2L}$	$\frac{(12W_{61}L - 12W_{62} + W_{53}L^2)}{12L}$	$\frac{(W_{11}L^2 + 3W_{22} - 3W_{21}L)}{3L}$
$\frac{(L(-2W_{02} + LW_{01} - W_{81}) + 2(W_{82} - W_{91}))}{2L}$	$\frac{(5L^2(-W_{87} + W_{07}L - W_{05}) + 60W_{96} + 6W_{85}L^2)}{5L^2}$	$\frac{(10L(W_{86} - W_{97}L - W_{95}) + 60W_{96} + 4W_{85}L^2)}{10L^2}$	$\frac{(L(2W_{02} - LW_{01} - W_{83}) + 2(W_{91} - W_{82}))}{2L}$
$\frac{(12(W_{92} - W_{91}L) + W_{81}L^2)}{12L}$	$\frac{(10L(-W_{86} - W_{97}L + W_{95}) + 60W_{96} + W_{85}L^2)}{10L^2}$	$\frac{(-15L(W_{86} + W_{95}) + 120W_{96} + 4W_{85}L^2)}{30L}$	$\frac{(12(-W_{92} + W_{91}L) + W_{81}L^2)}{12L}$
$\frac{(-6W_{22} + W_{11}L^2)}{6L}$	$\frac{(L(2W_{72} + W_{71}L - W_{51}) + 2(W_{61} - W_{52}))}{2L}$	$\frac{(-12W_{62} - W_{51}L^2)}{12L}$	$\frac{(12W_{22} + W_{11}L^2)}{12L}$
$\frac{(L(-2W_{72} + W_{71}L + W_{51}) + 2(W_{61} - W_{52}))}{2L}$	$\frac{(L^2(-6W_{55} + 5L^2W_{77}) - 60W_{66})}{5L^2}$	$\frac{(-L^2(10W_{76} + W_{55}) - 60W_{66})}{10L^2}$	$\frac{(L(2W_{72} - W_{71}L + W_{53}) - 2(W_{61} - W_{52}))}{2L}$
$\frac{(-12W_{62} - W_{51}L^2)}{12L}$	$\frac{(L^2(10W_{76} + W_{55}) + 60W_{66})}{10L^2}$	$\frac{(60W_{66} - W_{55}L^2)}{30L}$	$\frac{(12W_{62} - W_{53}L^2)}{12L}$
$\frac{(12W_{22} + W_{11}L^2)}{12L}$	$\frac{(L(-2W_{72} - LW_{71} - W_{53}) + 2(W_{52} - W_{61}))}{2L}$	$\frac{(12W_{62} - W_{53}L^2)}{12L}$	$\frac{(-6W_{22} + W_{11}L^2)}{6L}$
$\frac{(L(-2W_{02} + LW_{01} + W_{81}) + 2(W_{91} - W_{82}))}{2L}$	$\frac{(5L^2(W_{87} + W_{07}L - W_{05}) - 60W_{96} - 6W_{85}L^2)}{5L^2}$	$\frac{(10L(-W_{86} - W_{97}L + W_{95}) - 60W_{96} - W_{85}L^2)}{10L^2}$	$\frac{(L(2W_{02} - LW_{01} + W_{83}) - 2(W_{91} - W_{82}))}{2L}$
$\frac{(-12W_{92} - W_{81}L^2)}{12L}$	$\frac{(10L(W_{86} + W_{97}L - W_{95}) + 60W_{96} + W_{85}L^2)}{10L^2}$	$\frac{(15L(W_{86} - W_{95}) + 60W_{96} - W_{85}L^2)}{30L}$	$\frac{(12W_{92} - W_{83}L^2)}{12L}$

M₂=

M₂ - COLUMNS 5-8

$$\begin{array}{l}
 \frac{(L(-2W_{02} + LW_{01} - W_{81}) + 2(W_{82} - W_{91}))}{2L} \\
 \frac{(5L^2(-W_{87} + W_{07}L - W_{05}) + 60W_{96} + 6W_{85}L^2)}{5L^3} \\
 \frac{(10L(W_{86} - W_{97}L - W_{95}) + 60W_{96} + W_{85}L^2)}{10L^2} \\
 \frac{(L(2W_{02} - LW_{01} - W_{83}) + 2(W_{91} - W_{82}))}{2L} \\
 \frac{(L^2(6W_{88} - 10W_{08}L + 5W_{00}L^2) + 60W_{99})}{5L^3} \\
 \frac{(L^2(-10W_{09} + W_{88}) + 60W_{99})}{10L^2} \\
 \frac{(L(2W_{02} + LW_{01} - W_{81}) + 2(W_{91} - W_{82}))}{2L} \\
 \frac{(5L^2(-W_{87} + W_{07}L + W_{05}) - 60W_{96} - 6W_{85}L^2)}{5L^3} \\
 \frac{(10L(-W_{86} + W_{97}L + W_{95}) + 60W_{96} + W_{85}L^2)}{10L^2} \\
 \frac{(L(-2W_{02} - LW_{01} - W_{83}) - 2(W_{91} - W_{82}))}{2L} \\
 \frac{(L^2(-6W_{88} + 5L^2W_{00}) - 60W_{99})}{5L^3} \\
 \frac{(L^2(W_{88} + 10W_{09}) + 60W_{99})}{10L^2} \\
 \frac{(L(-2W_{02} - LW_{01} - W_{83}) - 2(W_{91} - W_{82}))}{2L} \\
 \frac{(L^2(-6W_{88} + 5L^2W_{00}) - 60W_{99})}{5L^3} \\
 \frac{(L^2(W_{88} + 10W_{09}) + 60W_{99})}{10L^2} \\
 \frac{(L(-2W_{02} + LW_{01} - W_{81}) + W_{81}L^2)}{12L} \\
 \frac{(10L(-W_{86} - W_{97}L + W_{95}) + 60W_{96} + W_{85}L^2)}{10L^2} \\
 \frac{(-15L(W_{86} + W_{95}) + 120W_{96} + 4W_{85}L^2)}{30L} \\
 \frac{(12(-W_{92} + W_{91}L) + W_{81}L^2)}{12L} \\
 \frac{(L^2(-10W_{09} + W_{88}) + 60W_{99})}{10L^2} \\
 \frac{(L(2W_{88}L - 15W_{98}) + 60W_{99})}{15L} \\
 \frac{(-12W_{92} - W_{81}L^2)}{12L} \\
 \frac{(10L(W_{86} - W_{97}L - W_{95}) - 60W_{96} - W_{85}L^2)}{10L^2} \\
 \frac{(15L(-W_{86} + W_{95}) + 60W_{96} - W_{85}L^2)}{30L} \\
 \frac{(12W_{92} - W_{83}L^2)}{12L} \\
 \frac{(-L^2(W_{88} + 10W_{09}) - 60W_{99})}{10L^2} \\
 \frac{(60W_{99} - W_{88}L^2)}{30L} \\
 \frac{(-6W_{22} + W_{11}L^2)}{6L} \\
 \frac{(L(2W_{72} + W_{71}L - W_{51}) + 2(W_{61} - W_{52}))}{2L} \\
 \frac{(-12W_{62} - W_{51}L^2)}{12L} \\
 \frac{(12W_{22} + W_{11}L^2)}{12L} \\
 \frac{(L(2W_{02} + LW_{01} - W_{81}) + 2(W_{91} - W_{82}))}{2L} \\
 \frac{(-12W_{92} - W_{81}L^2)}{12L} \\
 \frac{(L(3W_{21} + W_{11}L) + 3W_{22})}{3L} \\
 \frac{(L(2W_{72} + LW_{71} + W_{51}) - 2(W_{61} - W_{52}))}{2L} \\
 \frac{(12(W_{62} + W_{61}L) + W_{51}L^2)}{12L} \\
 \frac{(-6W_{21}L + W_{11}L^2 - 6W_{22})}{6L} \\
 \frac{(L(2W_{02} - LW_{01} + W_{81}) - 2(W_{91} - W_{82}))}{2L} \\
 \frac{(12(W_{92} + W_{91}L) + W_{81}L^2)}{12L} \\
 \frac{(L(-2W_{72} + W_{71}L + W_{51}) + 2(W_{61} - W_{52}))}{2L} \\
 \frac{(L^2(-6W_{55} + 5L^2W_{77}) - 60W_{66})}{5L^3} \\
 \frac{(-L^2(10W_{76} + W_{55}) - 60W_{66})}{10L^2} \\
 \frac{(L(2W_{72} - W_{71}L + W_{53}) - 2(W_{61} - W_{52}))}{2L} \\
 \frac{(5L^2(-W_{87} + W_{07}L + W_{05}) - 60W_{96} - 6W_{85}L^2)}{5L^3} \\
 \frac{(10L(W_{86} - W_{97}L - W_{95}) - 60W_{96} - W_{85}L^2)}{10L^2} \\
 \frac{(L(2W_{72} + LW_{71} + W_{51}) - 2(W_{61} - W_{52}))}{2L} \\
 \frac{(L^2(6W_{55} + 10W_{75}L + 5W_{77}L^2) + 60W_{66})}{5L^3} \\
 \frac{(L^2(-W_{55} + 10W_{76}) - 60W_{66})}{10L^2} \\
 \frac{(L(2W_{72} + W_{71}L - W_{53}) - 2(W_{61} - W_{52}))}{2L} \\
 \frac{(5L^3(W_{87} + W_{07}L + W_{05}) + 60W_{96} + 6W_{85}L^2)}{5L^3} \\
 \frac{(10L(-W_{86} + W_{97}L + W_{95}) - 60W_{96} - W_{85}L^2)}{10L^2}
 \end{array}$$

M₂ - COLUMNS 9-12

$\frac{(-12W_{62}-W_{51}L^2)}{12L}$	$\frac{(12W_{22}+W_{11}L^2)}{12L}$	$\frac{(L(-2W_{02}+LW_{01}+W_{81})+2(W_{91}-W_{82}))}{2L}$	$\frac{(-12W_{92}-W_{81}L^2)}{12L}$
$\frac{(L^2(10W_{76}+W_{55})+60W_{66})}{10L^2}$	$\frac{(L(-2W_{72}-LW_{71}-W_{53})+2(W_{52}-W_{61}))}{2L}$	$\frac{(5L^2(W_{87}+W_{07}L-W_{05})-60W_{96}-6W_{85}L^2)}{5L^3}$	$\frac{(10L(W_{86}+W_{97}L-W_{95})+60W_{96}+W_{85}L^2)}{10L^2}$
$\frac{(60W_{66}-W_{55}L^2)}{30L}$	$\frac{(12W_{62}-W_{53}L^2)}{12L}$	$\frac{(10L(-W_{86}-W_{97}L+W_{95})-60W_{96}-W_{85}L^2)}{10L^2}$	$\frac{(15L(W_{86}-W_{95})+60W_{96}-W_{85}L^2)}{30L}$
$\frac{(12W_{62}-W_{53}L^2)}{12L}$	$\frac{(-6W_{22}+W_{11}L^2)}{6L}$	$\frac{(L(2W_{02}-LW_{01}+W_{83})-2(W_{91}-W_{82}))}{2L}$	$\frac{(12W_{92}-W_{83}L^2)}{12L}$
$\frac{(10L(-W_{86}+W_{97}L+W_{95})+60W_{96}+W_{85}L^2)}{10L^2}$	$\frac{(L(-2W_{02}-LW_{01}-W_{83})-2(W_{91}-W_{82}))}{2L}$	$\frac{(L^2(-6W_{88}+5L^2W_{00})-60W_{99})}{5L^3}$	$\frac{(L^2(W_{88}+10W_{99})+60W_{99})}{10L^2}$
$\frac{(15L(-W_{86}+W_{95})+60W_{96}-W_{85}L^2)}{30L}$	$\frac{(12W_{92}-W_{83}L^2)}{12L}$	$\frac{(-L^2(W_{88}+10W_{99})-60W_{99})}{10L^2}$	$\frac{(60W_{99}-W_{88}L^2)}{30L}$
$\frac{(12(W_{62}+W_{61}L)+W_{51}L^2)}{12L}$	$\frac{(-6W_{21}L+W_{11}L^2-6W_{22})}{6L}$	$\frac{(L(2W_{02}-LW_{01}+W_{81})-2(W_{91}-W_{82}))}{2L}$	$\frac{(12(W_{92}+W_{91}L)+W_{81}L^2)}{12L}$
$\frac{(L^2(-W_{55}+10W_{76})-60W_{66})}{10L^2}$	$\frac{(L(2W_{72}+W_{71}L-W_{53})-2(W_{61}-W_{52}))}{2L}$	$\frac{(5L^2(W_{87}+W_{07}L+W_{05})+60W_{96}+6W_{85}L^2)}{5L^3}$	$\frac{(10L(-W_{86}+W_{97}L+W_{95})-60W_{96}-W_{85}L^2)}{10L^2}$
$\frac{(L(15W_{65}+2W_{55}L)+60W_{66})}{15L}$	$\frac{(-12(W_{62}+W_{61}L)+W_{53}L^2)}{12L}$	$\frac{(10L(W_{86}+W_{97}L-W_{95})-60W_{96}-W_{85}L^2)}{10L^2}$	$\frac{(15L(W_{86}+W_{95})+120W_{96}-4W_{85}L^2)}{30L}$
$\frac{(-12(W_{62}+W_{61}L)+W_{53}L^2)}{12L}$	$\frac{(3W_{21}L+W_{11}L^2+3W_{22})}{3L}$	$\frac{(-L(2W_{02}+LW_{01}-W_{83})+2(W_{91}-W_{82}))}{2L}$	$\frac{(-12(W_{92}+W_{91}L)+W_{83}L^2)}{12L}$
$\frac{(10L(W_{86}+W_{97}L-W_{95})-60W_{96}-W_{85}L^2)}{10L^2}$	$\frac{(-L(2W_{02}+LW_{01}-W_{83})+2(W_{91}-W_{82}))}{2L}$	$\frac{(L^2(6W_{88}+10W_{98}L+5W_{00}L^2)+60W_{99})}{5L^3}$	$\frac{(-L^2(W_{88}-10W_{99})-60W_{99})}{10L^2}$
$\frac{(15L(W_{86}+W_{95})+120W_{96}-4W_{85}L^2)}{30L}$	$\frac{(-12(W_{92}+W_{91}L)+W_{83}L^2)}{12L}$	$\frac{(-L^2(W_{88}-10W_{99})-60W_{99})}{10L^2}$	$\frac{(L(15W_{98}+2W_{88}L)+60W_{99})}{15L}$

where $W_{11} = \frac{hp}{3}$

$$\begin{aligned}
W_{21} &= \frac{-h^3 \rho}{96e} \\
W_{51} &= \frac{hp(4h_1 + h)}{24} \\
W_{81} &= \frac{-hp(2h_2 + h)}{24} \\
W_{82} &= \frac{-h^3 \rho h_2}{192e} \\
W_{65} &= \frac{-h^3 \rho h_1 (h_1 + h)}{384e} \\
W_{75} &= \frac{h^3 \rho h_1 (h_1 + h)}{1920e} \\
W_{76} &= \frac{-h^5 \rho (h_1 + h)^2}{15360e^2} \\
W_{87} &= \frac{h^3 \rho h_2 (h_1 + h)}{1920e} \\
W_{92} &= \frac{h^5 \rho (h_2 + h)}{1536e^2} \\
W_{02} &= \frac{-h^5 \rho (h_2 + h)}{7680e^2} \\
W_{97} &= \frac{-h^5 \rho (h_2 + h)(h_1 + h)}{15360e^2} \\
W_{07} &= \frac{h^5 \rho (h_2 + h)(h_1 + h)}{64512e^2} \\
W_{22} &= \frac{h^5 \rho}{768e^2} \\
W_{53} &= \frac{hp(2h_1 + h)}{24} \\
W_{52} &= \frac{-h^3 \rho h_1}{192e} \\
W_{61} &= \frac{-h^3 \rho (h_1 + h)}{192e} \\
W_{71} &= \frac{h^3 \rho (h_1 + h)}{960e} \\
W_{85} &= \frac{-hp(10h_1 h_2 + 5h_2 h + 5h_1 h + 2h^2)}{240} \\
W_{77} &= \frac{h^5 \rho (h_1 + h)^2}{64512e^2} \\
W_{88} &= \frac{hp(5h_2 h + 10h_2^2 + h^2)}{120} \\
W_{95} &= \frac{-h^3 \rho h_1 (h_2 + h)}{384e} \\
W_{05} &= \frac{h^3 \rho h_1 (h_2 + h)}{1920e} \\
W_{98} &= \frac{-h^3 \rho h_2 (h_2 + h)}{384e} \\
W_{08} &= \frac{h^3 \rho h_2 (h_2 + h)}{1920e} \\
W_{00} &= \frac{h^5 \rho (h_2 + h)^2}{64512e^2} \\
W_{83} &= \frac{-hp(4h_2 + h)}{24} \\
W_{55} &= \frac{hp(10h_1^2 + 5h_1 h + h^2)}{120} \\
W_{62} &= \frac{h^5 \rho (h_1 + h)}{1536e^2} \\
W_{72} &= \frac{-h^5 \rho (h_1 + h)}{7680e^2} \\
W_{66} &= \frac{h^5 \rho (h_1 + h)^2}{3072e^2} \\
W_{86} &= \frac{-h^3 \rho h_2 (h_1 + h)}{384e} \\
W_{91} &= \frac{-h^3 \rho (h_2 + h)}{192e} \\
W_{01} &= \frac{h^3 \rho (h_2 + h)}{960e} \\
W_{96} &= \frac{h^5 \rho (h_2 + h)(h_1 + h)}{3072e^2} \\
W_{99} &= \frac{h^5 \rho (h_2 + h)^2}{3072e^2} \\
W_{09} &= \frac{-h^5 \rho (h_2 + h)^2}{15360e^2}
\end{aligned}$$

APPENDIX 2

FORTRAN Program

```

PROGRAM SANDWICH
INTEGER BIT, ROW, COL, ICONNO(25)
REAL Mass(12,12),lth,Mmatrix(606,606),Imped
REAL K,L,ST1(12,12),M1(12,12),M2(12,12),M3(12,12)
COMPLEX Ec, C, D, E, F, G, H, Gc
COMPLEX Kmatrix(606,606), Si1,Si2
COMPLEX STIFFNESS(12, 12),ST2(12,12),ST3(12,12),ST4(12,12)
COMPLEX COMBINED(606,606), CINV(606,606)
COMPLEX Amatrix(606),Aconj

PRINT'(1X,A)'
PRINT'(1X,A)'
PRINT'(29X,A)!'SANDWICH BEAM ANALYSIS'
PRINT *,'
PRINT'(14X,A)!'Finite Element Model for 3-Layered Sandwich Beams'
PRINT '(1X,A)!'
PRINT *,'PLEASE ENTER THE NUMBER OF ELEMENTS TO BE USED'
READ *,NEL
PRINT *,'
PRINT*,'PLEASE ENTER VALUE FOR THE BEAM LENGTH (in INCHES):'
READ *,LTH
PRINT *,'BEAM LENGTH IS ',LTH,' inches'
PRINT *,'
PRINT*,'PLEASE ENTER VALUE FOR THE TOP FACE PLATE',
&' THICKNESS (in INCHES):'
READ *,H1
PRINT *,'TOP FACE THICKNESS IS ',H1,' inches'
PRINT *,'
PRINT*,'PLEASE ENTER VALUE FOR THE BOTTOM FACE PLATE',
&' THICKNESS (in INCHES):'
READ *,H2
PRINT *,'BOTTOM FACE THICKNESS IS ',H2,' inches'
PRINT *,'
PRINT*,'PLEASE ENTER VALUE FOR THE CORE THICKNESS (in INCHES):'
READ *,HH
PRINT *,'CORE THICKNESS IS ',HH,' inches'
PRINT *,'
PRINT*,'PLEASE ENTER VALUE FOR THE BEAM WIDTH (in INCHES):'

```

```

READ *,WW
PRINT *,'BEAM WIDTH IS ',WW,' inches'
PRINT *,''
* Beam Length (divided into elements)
lth = lth/REAL(nel)
PRINT *,'INPUT NUMBER OF CONSTRAINTS ON TOTAL BEAM'
READ *,NCONSTR
DO 25, ROW = 1,NCONSTR
PRINT *,'INPUT #',ROW,' ROW TO BE CONSTRAINED'
READ *, ICONNO(ROW)
25 CONTINUE
PRINT*,'INPUT MAGNITUDE OF POINT LOAD'
READ *,Fo
PRINT*,'LOAD MAGNITUDE IS ',Fo
PRINT*,'INPUT ROW NUMBER WHERE POINT LOAD IS APPLIED'
READ *,NMS
PRINT *,'TOP FACE PLATE MATERIAL IS (Choose one):'
PRINT '(35X,A)', '1. STEEL'
PRINT '(35X,A)', '2. OTHER'
READ *,BIT
IF (BIT .EQ. 1) THEN
CALL STEEL(r1,e1)
ELSE
CALL OTHER(r1,e1)
END IF
PRINT *,'BOTTOM FACE PLATE MATERIAL IS (Choose one):'
PRINT '(35X,A)', '1. STEEL'
PRINT '(35X,A)', '2. OTHER'
READ *,BIT
IF (BIT .EQ. 1) THEN
CALL STEEL(r2,e2)
ELSE
CALL OTHER(r2,e2)
END IF
PRINT *,'CORE MATERIAL IS (Choose one):'
PRINT '(35X,A)', '1. NEOPRENE'
PRINT '(35X,A)', '2. OTHER'
READ *,NET
IF (NET .EQ. 1) THEN
EVAL = 2.98
π = .000115
ELSE
PRINT*,'INPUT POISSONS RATIO:'
READ *,VC
PRINT*,'INPUT DENSITY:'

```

```

READ *,RR
EVAL = 2.0*(1.0+VC)
END IF

* mass density of steel multiplied by width of beam
r1 = r1*WW
r2 = r2*WW
* mass density of core (x width)
rr = rr*WW
*
E1 = E1*WW
E2 = E2*WW
A = (E1 * h1) / lth
B = (E2 * h2) / lth
K = (A * (h1 / lth) ** 2)
L = ((A * (h1 ** 2)) / 2.0 / lth)
P = ((A * (h1 ** 2)) / 3.0)
R = ((A * (h1 ** 2)) / 6.0)
S = (B * (h2 / lth) ** 2)
T = ((B * (h2 ** 2)) / 2.0 / lth)
W = ((B * (h2 ** 2)) / 3.0)
Y = ((B * (h2 ** 2)) / 6.0)
ALPHA=0.0

*23456789012345678902234567890323456789042345678905234567890623456789072

*Input Mass Matrix
CALL Mass1(hh,h1,h2,lth,rr,eval,M1)
CALL Mass2(hh,rr,eval,h1,h2,lth,Alpha,M2)
CALL Mass3(r1,r2,h1,h2,lth,M3)
DO 53, ROW=1,12
DO 54, COL=1,12
Mass(ROW,COL)=M1(ROW,COL)+M2(ROW,COL)+M3(ROW,COL)
54 continue
53 continue

*USE THIS COMMAND TO PRINT THE MASS MATRIX AND ITS COMPONENTS
* CALL WRRRN ('Mass-wc', 12, 12, M1, 12, 0)
* CALL WRRRN ('Mass-uc', 12, 12, M2, 12, 0)
* CALL WRRRN ('Mass-w & u', 12, 12, M3, 12, 0)
* CALL WRRRN ('Mass', 12, 12, Mass, 12, 0)

DO 3000, BIT=1,183

IF (BIT .LE. 50) THEN

```

```

    FREQ=BIT*2.0
    ELSE IF (BIT .LE. 75) THEN
        FREQ=(BIT-25.0)*4.0
    ELSE IF (BIT .LE. 85) THEN
        FREQ=(BIT-55.0)*10.0
    ELSE IF (BIT .LE. 120) THEN
        FREQ=(BIT-70.0)*20.0
    ELSE IF (BIT .LE. 145) THEN
        FREQ=(BIT-95.0)*40.0
    ELSE IF (BIT .LE. 183) THEN
        FREQ=(BIT-120.0)*80.0
    END IF
    IF (NET .EQ. 1) THEN
        CALL NEOPRENE(FREQ,RR,EC,VC)
    ELSE
        CALL OCORE(RR,EC)
    END IF
    IF (BIT .EQ. 1) THEN
        PRINT *, '          DENSITY    YOUNGS MODULUS',
        &'    POISSONS RATIO'
        PRINT '(30X,A),'REAL    IMAGINARY'
        PRINT 21,'TOP FACE    ',R1/ww,E1/ww
        PRINT 20,'CORE      ',RR,EC,'    ',VC
        PRINT 21,'BOTTOM FACE ',R2/ww,E2/ww
20  FORMAT (A16,E9.3,2 F13.3,A9,F4.2)
21  FORMAT (A16,E9.3,F13.3)
    END IF
    Ec=Ec*ww
    C = (13.0 * Ec * lth) / (35.0 * hh)
    D = (13.0 * Ec * (lth ** 2)) / (420.0 * hh)
    E = (11.0 * Ec * (lth ** 2)) / (210.0 * hh)
    F = (9.0 * Ec * lth) / (70.0 * hh)
    G = (Ec * (lth ** 3)) / (105.0 * hh)
    H = (Ec * (lth ** 3)) / (140.0 * hh)
    Gc = Ec/eval
    Si1=Gc/hh
    Si2=Ec*hh/12.0/(eval**2)

* Input Stiffness Matrix
    Call STIFF1(A,B,K,L,P,R,S,T,W,Y,ST1)
    Call STIFF2(C,D,E,F,G,H,ST2)
    Call STIFF3(Si1,hh,h1,h2,lth,ST3)
    Call STIFF4(Si2,hh,h1,h2,lth,ST4)
    DO 100, ROW=1,12
        DO 99, COL=1,12

```

```

      STIFFNESS(ROW,COL)=ST1(ROW,COL)+ST2(ROW,COL)+ST3(ROW,COL)
      STIFFNESS(ROW,COL)=STIFFNESS(ROW,COL)+ST4(ROW,COL)

```

```

99  continue

```

```

100 continue

```

```

* Add Elements FOR K MATRIX and M MATRIX

```

```

      Mdim=6*(nel+1)

```

```

      DO 1000, ROW=1,Mdim

```

```

        DO 1001, COL=1,Mdim

```

```

          Kmatrix(ROW,COL) = 0

```

```

          Mmatrix(ROW,COL) = 0

```

```

1001 continue

```

```

1000 CONTINUE

```

```

*USE THIS COMMAND TO PRINT THE STIFFNESS MATRIX AND ITS
COMPONENTS

```

```

      If (bit .eq. 1) then

```

```

*   CALL WRRRN ('K1 - u and w', 12, 12, St1, 12, 0)

```

```

*   CALL WRCRN ('K2 - phi', 12, 12, St2, 12, 0)

```

```

*   CALL WRCRN ('K3 - si', 12, 12, St3, 12, 0)

```

```

*   CALL WRCRN ('K4 - si x', 12, 12, St4, 12, 0)

```

```

*   Call WRCRN('STIFF',12,12,STIFFNESS,12,0)

```

```

      end if

```

```

      DO 1100, IEL=1,NEL

```

```

        IES= 6*(IEL-1)

```

```

        DO 1102, ROW = 1,12

```

```

          DO 1101, COL = 1,12

```

```

            IS = ROW + IES

```

```

            JS = COL + IES

```

```

            Kmatrix(IS,JS) = Kmatrix(IS,JS)+STIFFNESS(ROW,COL)

```

```

            Mmatrix(IS,JS) = Mmatrix(IS,JS)+Mass(ROW,COL)

```

```

1101 CONTINUE

```

```

1102 CONTINUE

```

```

1100 CONTINUE

```

```

* USE THIS COMMAND TO PRINT THE K AND M MATRICES

```

```

      IF (BIT .EQ. 1) THEN

```

```

        jed = 6*(nel+1)

```

```

*   Call WRCRN('Kmatrix',jed,jed,Kmatrix,606,0)

```

```

*   Call WRRRN('Mmatrix',jed,jed,Mmatrix,606,0)

```

```

      end if

```

```

      OMEGA= FREQ*2.0*3.141592654

```

```

*Combine Matrices
  DO 1200, ROW=1,Mdim
    DO 1200, COL=1,Mdim
      COMBINED(ROW,COL)=Kmatrix(ROW,COL)-
((OMEGA**2)*Mmatrix(ROW,COL))
1200 CONTINUE

*Boundary Conditions
  DO 1300, ICR=1,NCONSTR
    NR=ICONNO(ICR)
    DO 1400, ROW=1,Mdim
      COMBINED(ROW,NR)=0.0
      COMBINED(NR,ROW)=0.0
1400 CONTINUE
    COMBINED(NR,NR)=1.0
1300 CONTINUE

* Invert Combined Matrix
  CALL LINCG (Mdim,COMBINED,606,CINV,606)

* Multiply F and CINV

  DO 2000, ROW = 1,Mdim
    Amatrix(ROW) = CINV(ROW,NMS)*Fo
2000 CONTINUE
    Amatrix(NMS)=(Amatrix(NMS)+Amatrix(NMS+3))/2.0
    Aconj=CONJG(Amatrix(NMS))

* Calculate Impedance
  Imped=1.0/OMEGA/SQRT(Amatrix(NMS)*Aconj)

* Print Displacement Vector (For given values of freq)
*   If((FREQ.EQ.100.0).OR.(FREQ.EQ.160.0))THEN
*     Print *, ''
*     Print *, ' Peak #'
*     Print *,FREQ,Imped
*     DO 2001, Nog=1,Mdim
*       Print *, Amatrix(Nog)
*2001 continue
*     end if
* PRINT IMPEDANCE AND FREQ
  Print *,FREQ,Imped
3000 CONTINUE

  END

```

```
SUBROUTINE STEEL(R,E)
```

```
R=.000734
```

```
E= 29000000.0
```

```
END
```

```
SUBROUTINE OTHER(R,E)
```

```
PRINT*, 'INPUT DENSITY (LB*SEC(squared)/INCH(to the fourth):'
```

```
READ *,R
```

```
PRINT*, 'INPUT YOUNGS MODULUS:'
```

```
READ *,E
```

```
END
```

```
SUBROUTINE NEOPRENE(O,R,EC,V)
```

```
COMPLEX EC
```

```
*Poisson's Ratio
```

```
V = .49
```

```
* e
```

```
E = 2.0 * (1.0 + V)
```

```
E = E
```

```
* G
```

```
Shear1 = (2.7182818**(.026 * LOG (O) + 4.754))
```

```
* δ
```

```
Shear2 = (2.7182818**(.17 * LOG (O) - 2.705))
```

```
* Modulus for Core
```

```
EC = ((Shear1*E), (Shear1*Shear2*E))
```

```
* mass density of core
```

```
R = .000115
```

```
end
```

```
SUBROUTINE OCORE(R,EC)
```

```
COMPLEX EC
```

```
PRINT *, 'INPUT YOUNGS MODULUS (real, imaginary):'
```

```
READ *,EC
```

```
PRINT *, 'INPUT DENSITY:'
```

```
READ *,R
```

```
end
```

```
SUBROUTINE STIFF1(A,B,K,L,P,R,S,T,W,Y,STIFFNESS)
```

```
INTEGER ROW, COL
```

```
REAL STIFFNESS(12,12),L,K
```

```
* Input Stiffness Matrix
```

```
STIFFNESS(1, 1) = A
```

```

STIFFNESS(1, 7) = -A
STIFFNESS(2, 2) = K
STIFFNESS(2, 3) = L
STIFFNESS(2, 8) = -K
STIFFNESS(2, 9) = L
STIFFNESS(3, 3) = P
STIFFNESS(3, 8) = -L
STIFFNESS(3, 9) = R
STIFFNESS(4, 4) = B
STIFFNESS(4, 10) = -B
STIFFNESS(5, 5) = S
STIFFNESS(5, 6) = T
STIFFNESS(5, 11) = -S
STIFFNESS(5, 12) = T
STIFFNESS(6, 6) = W
STIFFNESS(6, 11) = -T
STIFFNESS(6, 12) = Y
STIFFNESS(7, 7) = A
STIFFNESS(8, 8) = K
STIFFNESS(8, 9) = -L
STIFFNESS(9, 9) = P
STIFFNESS(10, 10) = B
STIFFNESS(11, 11) = S
STIFFNESS(11, 12) = -T
STIFFNESS(12, 12) = W

```

```

DO 101, ROW=2,12
  IM1=ROW-1
  DO 101, COL= 1,IM1
    STIFFNESS(ROW,COL)=STIFFNESS(COL,ROW)
101 continue
end

```

```

SUBROUTINE STIFF2(C,D,E,F,G,H,STIFFNESS)
INTEGER ROW, COL
COMPLEX STIFFNESS(12,12),C,D,E,F,G,H
* Input Stiffness Matrix
STIFFNESS(2, 2) = C
STIFFNESS(2, 3) = E
STIFFNESS(2, 5) = -C
STIFFNESS(2, 6) = -E
STIFFNESS(2, 8) = F
STIFFNESS(2, 9) = -D
STIFFNESS(2, 11) = -F

```

```

STIFFNESS(2, 12)= D
STIFFNESS(3, 3) = G
STIFFNESS(3, 5) =-E
STIFFNESS(3, 6) =-G
STIFFNESS(3, 8) =D
STIFFNESS(3, 9) = -H
STIFFNESS(3, 11)=-D
STIFFNESS(3, 12) =H
STIFFNESS(5, 5) =C
STIFFNESS(5,6) =E
STIFFNESS(5,8) =-F
STIFFNESS(5,9) = D
STIFFNESS(5,11) =F
STIFFNESS(5,12)=-D
STIFFNESS(6, 6) =G
STIFFNESS(6, 8) = -D
STIFFNESS(6, 9) =H
STIFFNESS(6, 11) =D
STIFFNESS(6, 12) =-H
STIFFNESS(8,8)=C
STIFFNESS(8,9) =-E
STIFFNESS(8,11) =-C
STIFFNESS(8,12) =E
STIFFNESS(9,9) =G
STIFFNESS(9,11) =E
STIFFNESS(9,12) =-G
STIFFNESS(11, 11) =C
STIFFNESS(11, 12) =-E
STIFFNESS(12,12) =G

```

```

DO 102, ROW=2,12
  IM1=ROW-1
  DO 102, COL= 1,IM1
    STIFFNESS(ROW,COL)=STIFFNESS(COL,ROW)
102 continue
end

```

```

SUBROUTINE STIFF3(Si1,hh,h1,h2,lth,STIFFNESS)
INTEGER ROW, COL
REAL lth
COMPLEX STIFFNESS(12,12),Si1
Si2=0.0
* Input Stiffness Matrix
STIFFNESS(1, 1) = Si1 *lth/3.0+Si2*1.0/lth

```

$STIFFNESS(1, 2) = -Si1*(h1+hh)/4.0$
 $STIFFNESS(1, 3) = Si1*(h1+hh)/24.0*lth+Si2*(h1+hh)/2.0/lth$
 $STIFFNESS(1, 4) = -Si1*lth/3.0-Si2*1.0/lth$
 $STIFFNESS(1, 5) = -Si1*(h2+hh)/4.0$
 $STIFFNESS(1, 6) = Si1*(h2+hh)/24.0*lth+Si2*(h2+hh)/2.0/lth$
 $STIFFNESS(1, 7) = Si1*lth/6.0-Si2*1.0/lth$
 $STIFFNESS(1, 8) = Si1*(h1+hh)/4.0$
 $STIFFNESS(1, 9) = -Si1*(h1+hh)/24.0*lth-Si2*(h1+hh)/2.0/lth$
 $STIFFNESS(1, 10) = -Si1*lth/6.0+Si2*1.0/lth$
 $STIFFNESS(1, 11) = Si1*(h2+hh)/4.0$
 $STIFFNESS(1, 12) = -Si1*(h2+hh)/24.0*lth-Si2*(h2+hh)/2.0/lth$
 $STIFFNESS(2,2)=((h1+hh)**2)*(Si1*6.0/5.0/lth+Si2*12.0/(lth**3))$
 $STIFFNESS(2,2)=STIFFNESS(2,2)/4.0$
 $STIFFNESS(2,3)=((h1+hh)**2)/4.0*(Si1*1.0/10.0+Si2*6.0/(lth**2))$
 $STIFFNESS(2, 4) = Si1*(h1+hh)/4.0$
 $STIFFNESS(2,5)=(h1+hh)*(h2+hh)*(Si1*6.0/5.0/lth+Si2*12.0/(lth**3))$
 $STIFFNESS(2,5)=STIFFNESS(2,5)/4.0$
 $STIFFNESS(2,6)=(h1+hh)*(h2+hh)/4.0*(Si1*1.0/10.0+Si2*6.0/(lth**2))$
 $STIFFNESS(2,6)=STIFFNESS(2,6)$
 $STIFFNESS(2, 7) = -Si1*(h1+hh)/4.0$
 $STIFFNESS(2,8)=((h1+hh)**2)*(-Si1*6.0/5.0/lth-Si2*12.0/(lth**3))$
 $STIFFNESS(2,8)=STIFFNESS(2,8)/4.0$
 $STIFFNESS(2,9)=((h1+hh)**2)/4.0*(Si1*1.0/10.0+Si2*6.0/(lth**2))$
 $STIFFNESS(2, 10) = Si1*(h1+hh)/4.0$
 $STIFFNESS(2,11)=(h2+hh)/4.0*(-Si1*6.0/5.0/lth-Si2*12.0/(lth**3))$
 $STIFFNESS(2,11)=STIFFNESS(2,11)*(h1+hh)$
 $STIFFNESS(2,12)=(h1+hh)*(h2+hh)*(Si1*1.0/10.0+Si2*6.0/(lth**2))$
 $STIFFNESS(2,12)=STIFFNESS(2,12)/4.0$
 $STIFFNESS(3,3)=((h1+hh)**2)/4.0*(Si1*2.0/15.0*lth+Si2*4.0/lth)$
 $STIFFNESS(3, 4)=-Si1*(h1+hh)/24.0*lth-Si2*(h1+hh)/2.0/lth$
 $STIFFNESS(3,5)=STIFFNESS(2,12)$
 $STIFFNESS(3,6)=(h1+hh)*(h2+hh)/4.0*(Si1*2.0/15.0*lth+Si2*4.0/lth)$
 $STIFFNESS(3,6)=STIFFNESS(3,6)$
 $STIFFNESS(3,7) = -Si1*(h1+hh)/24.0*lth-Si2*(h1+hh)/2.0/lth$
 $STIFFNESS(3,8)=((h1+hh)**2)/4.0*(-Si1*1.0/10.0-Si2*6.0/(lth**2))$
 $STIFFNESS(3, 9) =((h1+hh)**2)/4.0*(-Si1*lth/30.0+Si2*2.0/lth)$
 $STIFFNESS(3, 10) =Si1*(h1+hh)/24.0*lth+Si2*(h1+hh)/2.0/lth$
 $STIFFNESS(3,11)=(h1+hh)*(h2+hh)*(-Si1*1.0/10.0-Si2*6.0/(lth**2))$
 $STIFFNESS(3,11)=STIFFNESS(3,11)/4.0$
 $STIFFNESS(3,12)=(h1+hh)*(h2+hh)/4.0*(-Si1*lth/30.0+Si2*2.0/lth)$
 $STIFFNESS(4, 4) =Si1*lth/3.0+Si2*1.0/lth$
 $STIFFNESS(4, 5) = Si1*(h2+hh)/4.0$
 $STIFFNESS(4, 6) = -Si2*(h2+hh)/2.0/lth-Si1*(h2+hh)/24.0*lth$
 $STIFFNESS(4, 7) = -Si1*lth/6.0+Si2*1.0/lth$
 $STIFFNESS(4, 8) = -Si1*(h1+hh)/4.0$

STIFFNESS(4, 9) = $Si2*(h1+hh)/2.0/lth+Si1*(h1+hh)/24.0*lth$
 STIFFNESS(4, 10) = $+Si1*lth/6.0-Si2*1.0/lth$
 STIFFNESS(4, 11) = $-Si1*(h2+hh)/4.0$
 STIFFNESS(4, 12) = $-STIFFNESS(4,6)$
 STIFFNESS(5,5) = $((h2+hh)**2)*(Si1*6.0/5.0/lth+Si2*12.0/(lth**3))$
 STIFFNESS(5,5) = $STIFFNESS(5,5)/4.0$
 STIFFNESS(5,6) = $((h2+hh)**2)/4.0*(Si1*1.0/10.0+Si2*6.0/(lth**2))$
 STIFFNESS(5, 7) = $-Si1*(h2+hh)/4.0$
 STIFFNESS(5, 8) = $STIFFNESS(2,11)$
 STIFFNESS(5, 9) = $STIFFNESS(2,12)$
 STIFFNESS(5, 10) = $Si1*(h2+hh)/4.0$
 STIFFNESS(5,11) = $((h2+hh)**2)*(-Si1*6.0/5.0/lth-Si2*12.0/(lth**3))$
 STIFFNESS(5,11) = $STIFFNESS(5,11)/4.0$
 STIFFNESS(5,12) = $((h2+hh)**2)/4.0*(Si1*1.0/10.0+Si2*6.0/(lth**2))$
 STIFFNESS(6,6) = $((h2+hh)**2)/4.0*(Si1*2.0/15.0*lth+Si2*4.0/lth)$
 STIFFNESS(6,7) = $-Si2*(h2+hh)/2.0/lth-Si1*(h2+hh)/24.0*lth$
 STIFFNESS(6, 8) = $STIFFNESS(3,11)$
 STIFFNESS(6, 9) = $STIFFNESS(3,12)$
 STIFFNESS(6, 10) = $Si2*(h2+hh)/2.0/lth+Si1*(h2+hh)/24.0*lth$
 STIFFNESS(6,11) = $((h2+hh)**2)/4.0*(-Si1*1.0/10.0-Si2*6.0/(lth**2))$
 STIFFNESS(6,11) = $STIFFNESS(6,11)$
 STIFFNESS(6, 12) = $((h2+hh)**2)/4.0*(-Si1*lth/30.0+Si2*2.0/lth)$
 STIFFNESS(7, 7) = $Si1*lth/3.0+Si2*1.0/lth$
 STIFFNESS(7, 8) = $Si1*(h1+hh)/4.0$
 STIFFNESS(7, 9) = $Si2*(h1+hh)/2.0/lth+Si1*(h1+hh)/24.0*lth$
 STIFFNESS(7, 10) = $-Si1*lth/3.0-Si2*1.0/lth$
 STIFFNESS(7, 11) = $Si1*(h2+hh)/4.0$
 STIFFNESS(7, 12) = $Si2*(h2+hh)/2.0/lth+Si1*(h2+hh)/24.0*lth$
 STIFFNESS(8, 8) = $STIFFNESS(2,2)$
 STIFFNESS(8, 9) = $STIFFNESS(3,8)$
 STIFFNESS(8, 10) = $-Si1*(h1+hh)/4.0$
 STIFFNESS(8, 11) = $STIFFNESS(2,5)$
 STIFFNESS(8, 12) = $STIFFNESS(3,11)$
 STIFFNESS(9, 9) = $STIFFNESS(3,3)$
 STIFFNESS(9, 10) = $-Si2*(h1+hh)/2.0/lth-Si1*(h1+hh)/24.0*lth$
 STIFFNESS(9, 11) = $STIFFNESS(8,12)$
 STIFFNESS(9, 12) = $STIFFNESS(3,6)$
 STIFFNESS(10, 10) = $Si1*lth/3.0+Si2*1.0/lth$
 STIFFNESS(10, 11) = $-Si1*(h2+hh)/4.0$
 STIFFNESS(10, 12) = $-Si2*(h2+hh)/2.0/lth-Si1*(h2+hh)/24.0*lth$
 STIFFNESS(11, 11) = $STIFFNESS(5,5)$
 STIFFNESS(11, 12) = $STIFFNESS(6,11)$
 STIFFNESS(12, 12) = $STIFFNESS(6,6)$

DO 103, ROW=2,12

```

      IM1=ROW-1
      DO 103, COL= 1,IM1
        STIFFNESS(ROW,COL)=STIFFNESS(COL,ROW)
103  continue
      end

      SUBROUTINE STIFF4(Si2,hh,h1,h2,lth,STIFFNESS)
      INTEGER ROW, COL
      REAL lth
      COMPLEX STIFFNESS(12,12),Si2
      Si1=0.0
* Input Stiffness Matrix
      STIFFNESS(1, 1) = Si1*lth/3.0+Si2*1.0/lth
      STIFFNESS(1, 2) = -Si1*(h1+hh)/4.0
      STIFFNESS(1, 3) = Si1*(h1+hh)/24.0*lth+Si2*(h1+hh)/2.0/lth
      STIFFNESS(1, 4) = -Si1*lth/3.0-Si2*1.0/lth
      STIFFNESS(1, 5) = -Si1*(h2+hh)/4.0
      STIFFNESS(1, 6) =Si1*(h2+hh)/24.0*lth+Si2*(h2+hh)/2.0/lth
      STIFFNESS(1, 7) = Si1*lth/6.0-Si2*1.0/lth
      STIFFNESS(1, 8) = Si1*(h1+hh)/4.0
      STIFFNESS(1, 9) = -Si1*(h1+hh)/24.0*lth-Si2*(h1+hh)/2.0/lth
      STIFFNESS(1, 10) = -Si1*lth/6.0+Si2*1.0/lth
      STIFFNESS(1, 11) = Si1*(h2+hh)/4.0
      STIFFNESS(1, 12) =-Si1*(h2+hh)/24.0*lth-Si2*(h2+hh)/2.0/lth
      STIFFNESS(2,2)=$((h1+hh)**2)*(Si1*6.0/5.0/lth+Si2*12.0/(lth**3))
      STIFFNESS(2,2)=STIFFNESS(2,2)/4.0
      STIFFNESS(2,3)=$((h1+hh)**2)/4.0*(Si1*1.0/10.0+Si2*6.0/(lth**2))
      STIFFNESS(2, 4) = Si1*(h1+hh)/4.0
      STIFFNESS(2,5)=$((h1+hh)*(h2+hh)*(Si1*6.0/5.0/lth+Si2*12.0/(lth**3))
      STIFFNESS(2,5)=STIFFNESS(2,5)/4.0
      STIFFNESS(2,6)=$((h1+hh)*(h2+hh)/4.0*(Si1*1.0/10.0+Si2*6.0/(lth**2))
      STIFFNESS(2,6)=STIFFNESS(2,6)
      STIFFNESS(2, 7) = -Si1*(h1+hh)/4.0
      STIFFNESS(2,8)=$((h1+hh)**2)*(-Si1*6.0/5.0/lth-Si2*12.0/(lth**3))
      STIFFNESS(2,8)=STIFFNESS(2,8)/4.0
      STIFFNESS(2,9)=$((h1+hh)**2)/4.0*(Si1*1.0/10.0+Si2*6.0/(lth**2))
      STIFFNESS(2, 10) = Si1*(h1+hh)/4.0
      STIFFNESS(2,11)=$((h2+hh)/4.0*(-Si1*6.0/5.0/lth-Si2*12.0/(lth**3))
      STIFFNESS(2,11)=STIFFNESS(2,11)*(h1+hh)
      STIFFNESS(2,12)=$((h1+hh)*(h2+hh)*(Si1*1.0/10.0+Si2*6.0/(lth**2))
      STIFFNESS(2,12)=STIFFNESS(2,12)/4.0
      STIFFNESS(3,3)=$((h1+hh)**2)/4.0*(Si1*2.0/15.0*lth+Si2*4.0/lth)
      STIFFNESS(3, 4)=-Si1*(h1+hh)/24.0*lth-Si2*(h1+hh)/2.0/lth
      STIFFNESS(3,5)=STIFFNESS(2,12)
      STIFFNESS(3,6)=$((h1+hh)*(h2+hh)/4.0*(Si1*2.0/15.0*lth+Si2*4.0/lth)

```

STIFFNESS(3,6)=STIFFNESS(3,6)
 STIFFNESS(3,7) = -Si1*(h1+hh)/24.0*lth-Si2*(h1+hh)/2.0/lth
 STIFFNESS(3,8)=\$((h1+hh)**2)/4.0*(-Si1*1.0/10.0-Si2*6.0/(lth**2))
 STIFFNESS(3,9)=\$((h1+hh)**2)/4.0*(-Si1*lth/30.0+Si2*2.0/lth)
 STIFFNESS(3,10) = Si1*(h1+hh)/24.0*lth+Si2*(h1+hh)/2.0/lth
 STIFFNESS(3,11)=\$((h1+hh)*(h2+hh)*(-Si1*1.0/10.0-Si2*6.0/(lth**2))
 STIFFNESS(3,11)=STIFFNESS(3,11)/4.0
 STIFFNESS(3,12)=\$((h1+hh)*(h2+hh)/4.0*(-Si1*lth/30.0+Si2*2.0/lth)
 STIFFNESS(4,4) = Si1*lth/3.0+Si2*1.0/lth
 STIFFNESS(4,5) = Si1*(h2+hh)/4.0
 STIFFNESS(4,6) = -Si2*(h2+hh)/2.0/lth-Si1*(h2+hh)/24.0*lth
 STIFFNESS(4,7) = -Si1*lth/6.0+Si2*1.0/lth
 STIFFNESS(4,8) = -Si1*(h1+hh)/4.0
 STIFFNESS(4,9) = Si2*(h1+hh)/2.0/lth+Si1*(h1+hh)/24.0*lth
 STIFFNESS(4,10) = +Si1*lth/6.0-Si2*1.0/lth
 STIFFNESS(4,11)=-Si1*(h2+hh)/4.0
 STIFFNESS(4,12) = -STIFFNESS(4,6)
 STIFFNESS(5,5)=\$((h2+hh)**2)*(Si1*6.0/5.0/lth+Si2*12.0/(lth**3))
 STIFFNESS(5,5)=STIFFNESS(5,5)/4.0
 STIFFNESS(5,6)=\$((h2+hh)**2)/4.0*(Si1*1.0/10.0+Si2*6.0/(lth**2))
 STIFFNESS(5,7) = -Si1*(h2+hh)/4.0
 STIFFNESS(5,8) = STIFFNESS(2,11)
 STIFFNESS(5,9) = STIFFNESS(2,12)
 STIFFNESS(5,10) = Si1*(h2+hh)/4.0
 STIFFNESS(5,11)=\$((h2+hh)**2)*(-Si1*6.0/5.0/lth-Si2*12.0/(lth**3))
 STIFFNESS(5,11)= STIFFNESS(5,11)/4.0
 STIFFNESS(5,12)=\$((h2+hh)**2)/4.0*(Si1*1.0/10.0+Si2*6.0/(lth**2))
 STIFFNESS(6,6)=\$((h2+hh)**2)/4.0*(Si1*2.0/15.0*lth+Si2*4.0/lth)
 STIFFNESS(6,7)=-Si2*(h2+hh)/2.0/lth-Si1*(h2+hh)/24.0*lth
 STIFFNESS(6,8) = STIFFNESS(3,11)
 STIFFNESS(6,9) = STIFFNESS(3,12)
 STIFFNESS(6,10) = Si2*(h2+hh)/2.0/lth+Si1*(h2+hh)/24.0*lth
 STIFFNESS(6,11)=\$((h2+hh)**2)/4.0*(-Si1*1.0/10.0-Si2*6.0/(lth**2))
 STIFFNESS(6,11)=STIFFNESS(6,11)
 STIFFNESS(6,12)=\$((h2+hh)**2)/4.0*(-Si1*lth/30.0+Si2*2.0/lth)
 STIFFNESS(7,7) = Si1*lth/3.0+Si2*1.0/lth
 STIFFNESS(7,8) = Si1*(h1+hh)/4.0
 STIFFNESS(7,9) = Si2*(h1+hh)/2.0/lth+Si1*(h1+hh)/24.0*lth
 STIFFNESS(7,10) = -Si1*lth/3.0-Si2*1.0/lth
 STIFFNESS(7,11) = Si1*(h2+hh)/4.0
 STIFFNESS(7,12) = Si2*(h2+hh)/2.0/lth+Si1*(h2+hh)/24.0*lth
 STIFFNESS(8,8) = STIFFNESS(2,2)
 STIFFNESS(8,9) = STIFFNESS(3,8)
 STIFFNESS(8,10) = -Si1*(h1+hh)/4.0
 STIFFNESS(8,11) = STIFFNESS(2,5)

```

STIFFNESS(8, 12) =STIFFNESS(3,11)
STIFFNESS(9, 9) =STIFFNESS(3,3)
STIFFNESS(9, 10)=-Si2*(h1+hh)/2.0/lth-Si1*(h1+hh)/24.0*lth
STIFFNESS(9, 11) =STIFFNESS(8,12)
STIFFNESS(9, 12) =STIFFNESS(3,6)
STIFFNESS(10, 10) =Si1*lth/3.0+Si2*1.0/lth
STIFFNESS(10, 11) = -Si1*(h2+hh)/4.0
STIFFNESS(10, 12) =-Si2*(h2+hh)/2.0/lth-Si1*(h2+hh)/24.0*lth
STIFFNESS(11, 11) =STIFFNESS(5,5)
STIFFNESS(11, 12) =STIFFNESS(6,11)
STIFFNESS(12, 12) = STIFFNESS(6,6)

DO 104, ROW=2,12
  IM1=ROW-1
  DO 104, COL= 1,IM1
    STIFFNESS(ROW,COL)=STIFFNESS(COL,ROW)
104 continue
end

SUBROUTINE Mass1(hh,h1,h2,lth,rr,eval,Mass)
INTEGER ROW, COL
REAL lth, Mass(12,12)

U16=rr*(6.0*hh*(h1+hh)-5.0*eval*(lth**2))
U16=U16*((hh/eval)**2)/1440.0/lth
U55=42.0*hh*h1*((hh**2)-eval*(lth**2)+hh*h1/2.0)+21.0*(hh**4)
U55=U55+104.0*(eval**2)*(lth**4)-42.0*eval*((hh*lth)**2)
U55=U55*hh*rr/840.0/(lth**3)/(eval**2)
U56=126.0*hh*h1*((hh**2)-eval*(lth**2)+hh*h1/2.0)+63.0*(hh**4)
U56=U56+88.0*(eval**2)*(lth**4)-126.0*eval*((hh*lth)**2)
U56=U56*hh*rr/5040.0/(lth**2)/(eval**2)
U57=14.0*hh*h1*((hh**2)-eval*(lth**2)+hh*h1/2.0)+7.0*(hh**4)
U57=U57-12.0*(eval**2)*(lth**4)-14.0*eval*((hh*lth)**2)
U57=U57*(-hh)*rr/280.0/(lth**3)/(eval**2)
U58=126.0*hh*h1*((hh**2)-eval*(lth**2)/6.0+hh*h1/2.0)+63.0*(hh**4)
U58=U58-52.0*(eval**2)*(lth**4)-21.0*eval*((hh*lth)**2)
U58=U58*hh*rr/5040.0/(lth**2)/(eval**2)
U66=42.0*hh*h1*((hh**2)-eval*(lth**2)/3.0+hh*h1/2.0)+21.0*(hh**4)
U66=U66+8.0*(eval**2)*(lth**4)-14.0*eval*((hh*lth)**2)
U66=U66*hh*rr/2520.0/(lth)/(eval**2)
U00=42.0*hh*h2*((hh**2)-eval*(lth**2)/3.0+hh*h2/2.0)+21.0*(hh**4)
U00=U00+8.0*(eval**2)*(lth**4)-14.0*eval*((hh*lth)**2)
U00=U00*hh*rr/2520.0/(lth)/(eval**2)
U10=126.0*hh*h2*(eval*(lth**2)/6.0-(hh**2)-hh*h2/2.0)-63.0*(hh**4)
U10=U10+52.0*(eval**2)*(lth**4)+21.0*eval*((hh*lth)**2)

```

$$U10=U10*hh*rr/5040.0/(lth**2)/(eval**2)$$

$$U68=42.0*hh*h1*((hh**2)+eval*(lth**2))/6.0+hh*h1/2.0)+21.0*(hh**4)$$

$$U68=U68-12.0*(eval**2)*(lth**4)+7.0*eval*((hh*lth)**2)$$

$$U68=U68*hh*rr/5040.0/(lth)/(eval**2)$$

$$U99=42.0*hh*h2*((hh**2)-eval*(lth**2)+hh*h2/2.0)+21.0*(hh**4)$$

$$U99=U99+104.0*(eval**2)*(lth**4)-42.0*eval*((hh*lth)**2)$$

$$U99=U99*hh*rr/840.0/(lth**3)/(eval**2)$$

$$U90=126.0*hh*h2*((hh**2)-eval*(lth**2)+hh*h2/2.0)+63.0*(hh**4)$$

$$U90=U90+88.0*(eval**2)*(lth**4)-126.0*eval*((hh*lth)**2)$$

$$U90=U90*hh*rr/5040.0/(lth**2)/(eval**2)$$

$$U91=14.0*hh*h2*((hh**2)-eval*(lth**2)+hh*h2/2.0)+7.0*(hh**4)$$

$$U91=U91-12.0*(eval**2)*(lth**4)-14.0*eval*((hh*lth)**2)$$

$$U91=U91*(-hh)*rr/280.0/(lth**3)/(eval**2)$$

$$U11=42.0*hh*h2*((hh**2)+eval*(lth**2))/6.0+hh*h2/2.0)+21.0*(hh**4)$$

$$U11=U11-12.0*(eval**2)*(lth**4)+7.0*eval*((hh*lth)**2)$$

$$U11=U11*hh*rr/5040.0/(lth)/(eval**2)$$

$$U59=21.0*hh*(hh*h1*h2-eval*h1*(lth**2)+(hh**3)+h2*hh*hh+h1*hh*hh)$$

$$U59=U59+52.0*(eval**2)*(lth**4)-21.0*hh*eval*h2*(lth**2)$$

$$U59=(U59-42.0*eval*((hh*lth)**2))*hh*rr/840.0/(lth**3)/(eval**2)$$

$$U69=126.0*hh*(hh*h1*h2-eval*h2*(lth**2))/6.0+(hh**3)+h2*hh*hh)$$

$$U69=U69+88.0*(eval**2)*(lth**4)-231.0*hh*eval*h1*(lth**2)$$

$$U69=U69+126.0*(hh**3)*h1-252.0*eval*((hh*lth)**2)$$

$$U69=U69*hh*rr/10080.0/(lth**2)/(eval**2)$$

$$U79=7.0*hh*(eval*h1*(lth**2)-hh*h1*h2-(hh**3)-h2*hh*hh-h1*hh*hh)$$

$$U79=U79+6.0*(eval**2)*(lth**4)+7.0*hh*eval*h2*(lth**2)$$

$$U79=(U79+14.0*eval*((hh*lth)**2))*hh*rr/280.0/(lth**3)/(eval**2)$$

$$U89=126.0*hh*(hh*h1*h2-eval*h2*(lth**2))/6.0+(hh**3)+h2*hh*hh)$$

$$U89=U89-52.0*(eval**2)*(lth**4)-21.0*hh*eval*h1*(lth**2)$$

$$U89=U89+126.0*(hh**3)*h1-42.0*eval*((hh*lth)**2)$$

$$U89=U89*hh*rr/10080.0/(lth**2)/(eval**2)$$

$$U50=126.0*hh*(hh*h1*h2-eval*h1*(lth**2))/6.0+(hh**3)+h2*hh*hh)$$

$$U50=U50+88.0*(eval**2)*(lth**4)-231.0*hh*eval*h2*(lth**2)$$

$$U50=U50-252.0*eval*((hh*lth)**2)+126.0*(hh**3)*h1$$

$$U50=U50*hh*rr/10080.0/(lth**2)/(eval**2)$$

$$U60=21.0*hh*(hh*h1*h2-eval*h2*(lth**2))/3.0+(hh**3)+h2*hh*hh)$$

$$U60=U60+4.0*(eval**2)*(lth**4)-7.0*hh*eval*h1*(lth**2)$$

$$U60=U60+21.0*(hh**3)*h1-14.0*eval*((hh*lth)**2)$$

$$U60=U60*hh*rr/2520.0/(lth)/(eval**2)$$

$$U80=42.0*hh*(eval*h1*(lth**2))/6.0+hh*h1*h2+(hh**3)+h2*hh*hh)$$

$$U80=U80-12.0*(eval**2)*(lth**4)+7.0*hh*eval*h2*(lth**2)$$

$$U80=U80+14.0*eval*((hh*lth)**2)+42.0*(hh**3)*h1$$

$$U80=U80*hh*rr/10080.0/(lth)/(eval**2)$$

$$Mass(1,1)=rr*(hh**3)/120.0/lth/(eval**2)$$

$$Mass(1,7)=-rr*(hh**3)/120.0/lth/(eval**2)$$

$$Mass(1,4)=-rr*(hh**3)/120.0/lth/(eval**2)$$

Mass(1,10)=rr*(hh**3)/120.0/lth/(eval**2)
 Mass(1,2)=-rr*(hh**2)/48.0/eval
 Mass(1,3)=U16
 Mass(1,8)=-rr*(hh**2)/48.0/eval
 Mass(1,9)=-U16
 Mass(1,5)=-rr*(hh**2)/48.0/eval
 Mass(1,6)=U16
 Mass(1,11)=-rr*(hh**2)/48.0/eval
 Mass(1,12)=-U16
 Mass(7,7)=rr*(hh**3)/120.0/lth/(eval**2)
 Mass(4,7)=rr*(hh**3)/120.0/lth/(eval**2)
 Mass(7,10)=-rr*(hh**3)/120.0/lth/(eval**2)
 Mass(2,7)=rr*(hh**2)/48.0/eval
 Mass(3,7)=-U16
 Mass(7,8)=rr*(hh**2)/48.0/eval
 Mass(7,9)=U16
 Mass(5,7)=rr*(hh**2)/48.0/eval
 Mass(6,7)=-U16
 Mass(7,11)=rr*(hh**2)/48.0/eval
 Mass(7,12)=U16
 Mass(4,4)=rr*(hh**3)/120.0/lth/(eval**2)
 Mass(4,10)=-rr*(hh**3)/120.0/lth/(eval**2)
 Mass(2,4)=rr*(hh**2)/48.0/eval
 Mass(3,4)=-U16
 Mass(4,8)=rr*(hh**2)/48.0/eval
 Mass(4,9)=U16
 Mass(4,5)=rr*(hh**2)/48.0/eval
 Mass(4,6)=-U16
 Mass(4,11)=rr*(hh**2)/48.0/eval
 Mass(4,12)=U16
 Mass(10,10)=rr*(hh**3)/120.0/lth/(eval**2)
 Mass(2,10)=-rr*(hh**2)/48.0/eval
 Mass(3,10)=U16
 Mass(8,10)=-rr*(hh**2)/48.0/eval
 Mass(9,10)=-U16
 Mass(5,10)=-rr*(hh**2)/48.0/eval
 Mass(6,10)=U16
 Mass(10,11)=-rr*(hh**2)/48.0/eval
 Mass(10,12)=-U16
 Mass(2,2)=U55
 Mass(2,3)=U56
 Mass(2,8)=U57
 Mass(2,9)=U58
 Mass(2,5)=U59
 Mass(2,6)=U50

```

Mass(2,11)=U79
Mass(2,12)=U89
Mass(3,3)=U66
Mass(3,8)=-U58
Mass(3,9)=U68
Mass(3,5)=U69
Mass(3,6)=U60
Mass(3,11)=-U89
Mass(3,12)=U80
Mass(8,8)=U55
Mass(8,9)=-U56
Mass(5,8)=U79
Mass(6,8)=-U89
Mass(8,11)=U59
Mass(8,12)=-U50
Mass(9,9)=U66
Mass(5,9)=U89
Mass(6,9)=U80
Mass(9,11)=-U69
Mass(9,12)=U60
Mass(5,5)=U99
Mass(5,6)=U90
Mass(5,11)=U91
Mass(5,12)=-U10
Mass(6,6)=U00
Mass(6,11)=U10
Mass(6,12)=U11
Mass(11,11)=U99
Mass(11,12)=-U90
Mass(12,12)=U00
DO 50, ROW=2,12
  IM1=ROW-1
  DO 50, COL= 1,IM1
    Mass(row,col)=Mass(col,row)
50 continue
end

SUBROUTINE Mass2(hh,rr,eval,h1,h2,lth,Alpha,Mass)
INTEGER ROW, COL
REAL Mas(12,12),Mass(12,12),lth
W11 =1.0/3.0*hh*rr
W21=-1.0/96.0*(hh**3)/eval*rr
W22 =1.0/768.0*(hh**5)/(eval**2)*rr
W51=1.0/24.0*hh*(4.0*h1+hh)*rr
W53 =1.0/24.0*hh*(2.0*h1+hh)*rr

```

$W83 = -1.0/24.0*hh*(4.0*h2+hh)*rr$
 $W81 = -1.0/24.0*hh*(2.0*h2+hh)*rr$
 $W52 = -1.0/192.0*(hh**3)*h1/eval*rr$
 $W55=1.0/120.0*hh*(10.0*(h1**2)+5.0*h1*hh+(hh**2))*rr$
 $W82 = -1.0/192.0*(hh**3)*h2/eval*rr$
 $W61=-1.0/192.0*(h1+hh)*(hh**3)*rr/eval$
 $W62=1.0/1536.0*(hh**5)*(h1+hh)/(eval**2)*rr$
 $W65=-1.0/384.0*(h1+hh)*(hh**3)*h1*rr/eval$
 $W71=1.0/960.0*(h1+hh)*(hh**3)*rr/eval$
 $W72=-1.0/7680.0*(hh**5)*(h1+hh)/(eval**2)*rr$
 $W75=1.0/1920.0*(h1+hh)*(hh**3)*h1*rr/eval$
 $W85=-1.0/240.0*hh*(2.0*(hh**2)+5.0*hh*(h1+h2)+10.0*h1*h2)*rr$
 $W66=1.0/3072.0*(hh**5)*((h1+hh)**2)/(eval**2)*rr$
 $W76=-1.0/15360.0*(hh**5)*((h1+hh)**2)/(eval**2)*rr$
 $W77=1.0/64512.0*(hh**5)*((h1+hh)**2)/(eval**2)*rr$
 $W86=-1.0/384.0*(h1+hh)*(hh**3)*h2*rr/eval$
 $W87=1.0/1920.0*(h1+hh)*(hh**3)*h2*rr/eval$
 $W88=1.0/120.0*hh*((hh**2)+5.0*hh*h2+10.0*(h2**2))*rr$
 $W91=-1.0/192.0*(h2+hh)*(hh**3)*rr/eval$
 $W92=1.0/1536.0*(hh**5)*(h2+hh)/(eval**2)*rr$
 $W95=-1.0/384.0*(h2+hh)*(hh**3)*h1*rr/eval$
 $W01=1.0/960.0*(h2+hh)*(hh**3)*rr/eval$
 $W02=-1.0/7680.0*(hh**5)*(h2+hh)/(eval**2)*rr$
 $W05=1.0/1920.0*(h2+hh)*(hh**3)*h1*rr/eval$
 $W96=1.0/3072.0*(hh**5)*(h1+hh)*(h2+hh)/(eval**2)*rr$
 $W97=-1.0/15360.0*(hh**5)*(h1+hh)*(h2+hh)/(eval**2)*rr$
 $W98=-1.0/384.0*(h2+hh)*(hh**3)*h2*rr/eval$
 $W99=1.0/3072.0*(hh**5)*((h2+hh)**2)/(eval**2)*rr$
 $W07=1.0/64512.0*(hh**5)*(h1+hh)*(h2+hh)/(eval**2)*rr$
 $W08=1.0/1920.0*(h2+hh)*(hh**3)*h2*rr/eval$
 $W09=-1.0/15360.0*(hh**5)*((h2+hh)**2)/(eval**2)*rr$
 $W00=1.0/64512.0*(hh**5)*((h2+hh)**2)/(eval**2)*rr$
 $Mas(1,1)=(-1.0/3.0/lth*(-W11*(lth**2)-3.0*W22+3.0*W21*lth))$
 $Mas(1,2)=1.0/6.0/lth*(-6.0*W22+W11*(lth**2))$
 $Mas(1,3)=1.0/6.0/lth*(W11*(lth**2)+6.0*W21*lth-6.0*W22)$
 $Mas(1,4)=1.0/6.0/lth*(W11/2.0*(lth**2)+W22*6.0)$
 $Mas(1,5)=ALPHA*lth*(-2.0*W72+lth*W71)-lth*W51+2.0*(W52-W61)$
 $Mas(1,5)=1.0/2.0/lth*Mas(1,5)$
 $Mas(1,6)=1.0/12.0/lth*(12.0*(W62-W61*lth)+W51*(lth**2))$
 $Mas(1,7)=ALPHA*lth*(-2.0*W72+lth*W71)+lth*W51+2.0*(W61-W52)$
 $Mas(1,7)=1.0/2.0/lth*Mas(1,7)$
 $Mas(1,8)=-1.0/12.0/lth*(12.0*W62+W51*(lth**2))$
 $Mas(1,9)=ALPHA*lth*(-2.0*W02+lth*W01)-lth*W81+2.0*(W82-W91)$
 $Mas(1,9)=1.0/2.0/lth*Mas(1,9)$
 $Mas(1,10)=1.0/12.0/lth*(12.0*(W92-W91*lth)+W81*(lth**2))$

$Mas(1,11)=ALPHA*lth*(-2.0*W02+lth*W01)+lth*W81+2.0*(W91-W82)$
 $Mas(1,11)=1.0/2.0/lth*Mas(1,11)$
 $Mas(1,12)=-1.0/12.0/lth*(12.0*W92+W81*(lth**2))$
 $Mas(2,2)=(1.0/3.0/lth*(W11*(lth**2)+3.0*W22+3.0*W21*lth))$
 $Mas(2,3)=Mas(1,4)$
 $Mas(2,4)=1.0/6.0/lth*(W11*(lth**2)-6.0*W21*lth-6.0*W22)$
 $Mas(2,5)=ALPHA*lth*(2.0*W72+lth*W71)-lth*W51-2.0*(W52-W61)$
 $Mas(2,5)=1.0/2.0/lth*Mas(2,5)$
 $Mas(2,6)=Mas(1,8)$
 $Mas(2,7)=ALPHA*lth*(2.0*W72+lth*W71)+lth*W51+2.0*(W52-W61)$
 $Mas(2,7)=1.0/2.0/lth*Mas(2,7)$
 $Mas(2,8)=1.0/12.0/lth*(12.0*(W62+W61*lth)+W51*(lth**2))$
 $Mas(2,9)=ALPHA*lth*(2.0*W02+lth*W01)-lth*W81+2.0*(W91-W82)$
 $Mas(2,9)=1.0/2.0/lth*Mas(2,9)$
 $Mas(2,10)=Mas(1,12)$
 $Mas(2,11)=ALPHA*lth*(2.0*W02+lth*W01)+lth*W81-2.0*(W91-W82)$
 $Mas(2,11)=1.0/2.0/lth*Mas(2,11)$
 $Mas(2,12)=1.0/12.0/lth*(12.0*(W92+W91*lth)+W81*(lth**2))$
 $Mas(3,3)=Mas(1,1)$
 $Mas(3,4)=Mas(1,2)$
 $Mas(3,5)=ALPHA*lth*(-2.0*W72+lth*W71)+lth*W53+2.0*(W52-W61)$
 $Mas(3,5)=-1.0/2.0/lth*Mas(3,5)$
 $Mas(3,6)=1.0/12.0/lth*(12.0*(-W62+W61*lth)+W53*(lth**2))$
 $Mas(3,7)=ALPHA*lth*(-2.0*W72+lth*W71)-lth*W53+2.0*(W61-W52)$
 $Mas(3,7)=-1.0/2.0/lth*Mas(3,7)$
 $Mas(3,8)=1.0/12.0/lth*(12.0*W62-W53*(lth**2))$
 $Mas(3,9)=ALPHA*lth*(-2.0*W02+lth*W01)+lth*W83+2.0*(W82-W91)$
 $Mas(3,9)=-1.0/2.0/lth*Mas(3,9)$
 $Mas(3,10)=-1.0/12.0/lth*(12.0*(W92-W91*lth)-W83*(lth**2))$
 $Mas(3,11)=ALPHA*lth*(-2.0*W02+lth*W01)-lth*W83+2.0*(W91-W82)$
 $Mas(3,11)=-1.0/2.0/lth*Mas(3,11)$
 $Mas(3,12)=1.0/12.0/lth*(12.0*W92-W83*(lth**2))$
 $Mas(4,4)=Mas(2,2)$
 $Mas(4,5)=ALPHA*lth*(2.0*W72+lth*W71)+lth*W53-2.0*(W52-W61)$
 $Mas(4,5)=-1.0/2.0/lth*Mas(4,5)$
 $Mas(4,6)=Mas(3,8)$
 $Mas(4,7)=ALPHA*lth*(2.0*W72+lth*W71)-lth*W53+2.0*(W52-W61)$
 $Mas(4,7)=-1.0/2.0/lth*Mas(4,7)$
 $Mas(4,8)=-1.0/12.0/lth*(12.0*(W62+W61*lth)-W53*(lth**2))$
 $Mas(4,9)=ALPHA*lth*(2.0*W02+lth*W01)+lth*W83+2.0*(W91-W82)$
 $Mas(4,9)=-1.0/2.0/lth*Mas(4,9)$
 $Mas(4,10)=Mas(3,12)$
 $Mas(4,11)=ALPHA*lth*(2.0*W02+lth*W01)-lth*W83-2.0*(W91-W82)$
 $Mas(4,11)=-1.0/2.0/lth*Mas(4,11)$
 $Mas(4,12)=-1.0/12.0/lth*(12.0*(W92+W91*lth)-W83*(lth**2))$

$Mas(5,5)=ALPHA*(lth^{**3})*5.0*(-2.0*W75+lth*W77*ALPHA)+60.0*W66$
 $Mas(5,5)=1.0/5.0/(lth^{**3})*(Mas(5,5)+6.0*W55*(lth^{**2}))$
 $Mas(5,6)=-1.0/10.0*(10.0*W76*ALPHA-W55-W66*60.0/(lth^{**2}))$
 $Mas(5,7)=(ALPHA^{**2})*W77*(lth^{**4})*5.0-W55*6.0*(lth^{**2})-W66*60.0$
 $Mas(5,7)=1.0/5.0/(lth^{**3})*Mas(5,7)$
 $Mas(5,8)=1.0/10.0*(10.0*W76*ALPHA+W55+W66*60.0/(lth^{**2}))$
 $Mas(5,10)=W95/lth-ALPHA*W97-W86/lth+W85/10.0+6.0*W96/(lth^{**2})$
 $Mas(5,9)=ALPHA*(ALPHA*lth*W07-W05-W87)+6.0*W85/lth/5.0$
 $Mas(5,9)=Mas(5,9)+60.0*W96/(lth^{**3})/5.0$
 $Mas(5,11)=ALPHA*(ALPHA*lth*W07-W05+W87)-6.0*W85/lth/5.0$
 $Mas(5,11)=Mas(5,11)-60.0*W96/(lth^{**3})/5.0$
 $Mas(5,12)=ALPHA*W97-(W95-W86)/lth+W85/10.0+6.0*W96/(lth^{**2})$
 $Mas(6,6)=(4.0*W66-W65*lth+2.0/15.0*W55*(lth^{**2}))/lth$
 $Mas(6,7)=-Mas(5,8)$
 $Mas(6,8)=(60.0*W66-W55*(lth^{**2}))/30.0/lth$
 $Mas(6,9)=ALPHA*(-W97)-(W95-W86)/lth+W85/10.0+6.0*W96/(lth^{**2})$
 $Mas(6,12)=2.0*W96/lth-1.0/30.0*W85*lth+(W86-W95)/2.0$
 $Mas(6,11)=(W95-W86)/lth-ALPHA*W97-W85/10.0-6.0*W96/(lth^{**2})$
 $Mas(6,10)=4.0*W96/lth+4.0/30.0*W85*lth-(W86+W95)/2.0$
 $Mas(7,7)=(ALPHA^{**2})*W77*lth+W55*6.0/5.0/lth+W66*12.0/(lth^{**3})$
 $Mas(7,7)=Mas(7,7)+2.0*W75*ALPHA$
 $Mas(7,8)=1.0/10.0*(10.0*W76*ALPHA-W55-W66*60.0/(lth^{**2}))$
 $Mas(7,10)=W86/lth-ALPHA*W97-W95/lth-W85/10.0-6.0*W96/(lth^{**2})$
 $Mas(7,9)=ALPHA*(ALPHA*lth*W07+W05-W87)-6.0*W85/lth/5.0$
 $Mas(7,9)=Mas(7,9)-60.0*W96/(lth^{**3})/5.0$
 $Mas(7,11)=ALPHA*(ALPHA*lth*W07+W05+W87)+6.0*W85/lth/5.0$
 $Mas(7,11)=Mas(7,11)+60.0*W96/(lth^{**3})/5.0$
 $Mas(7,12)=ALPHA*W97+(W95-W86)/lth-W85/10.0-6.0*W96/(lth^{**2})$
 $Mas(8,8)=(4.0*W66+W65*lth+2.0/15.0*W55*(lth^{**2}))/lth$
 $Mas(8,9)=ALPHA*W97+(W95-W86)/lth+W85/10.0+6.0*W96/(lth^{**2})$
 $Mas(8,10)=2.0*W96/lth-1.0/30.0*W85*lth-(W86-W95)/2.0$
 $Mas(8,11)=(W86-W95)/lth+ALPHA*W97-W85/10.0-6.0*W96/(lth^{**2})$
 $Mas(8,12)=4.0*W96/lth+4.0/30.0*W85*lth+(W86+W95)/2.0$
 $Mas(9,9)=lth*(ALPHA^{**2})*W00-2.0*ALPHA*W08+12.0*W99/(lth^{**3})$
 $Mas(9,9)=Mas(9,9)+6.0/5.0*W88/lth$
 $Mas(9,10)=W99*6.0/(lth^{**2})-W09*ALPHA+W88/10.0$
 $Mas(9,11)=W00*(ALPHA^{**2})*lth-W99*12.0/(lth^{**3})-W88*6.0/5.0/lth$
 $Mas(9,11)=Mas(9,11)$
 $Mas(9,12)=W09*ALPHA+W88/10.0+6.0*W99/(lth^{**2})$
 $Mas(10,10)=4.0*W99/lth-W98+2.0/15.0*W88*lth$
 $Mas(10,11)=-Mas(9,12)$
 $Mas(10,12)=2.0*W99/lth-W88*lth/30.0$
 $Mas(11,11)=ALPHA*(2.0*W08+ALPHA*lth*W00)+12.0*W99/(lth^{**3})$
 $Mas(11,11)=Mas(11,11)+6.0/5.0*W88/lth$
 $Mas(11,12)=W09*ALPHA-6.0*W99/(lth^{**2})-W88/10.0$

Mass(12,12)=W98+4.0*W99/lth+2.0/15.0*W88*lth
Mass(1,1)=Mas(1,1)
Mass(1,7)=Mas(1,2)
Mass(1,4)=Mas(1,3)
Mass(1,10)=Mas(1,4)
Mass(1,2)=Mas(1,5)
Mass(1,3)=Mas(1,6)
Mass(1,8)=Mas(1,7)
Mass(1,9)=Mas(1,8)
Mass(1,5)=Mas(1,9)
Mass(1,6)=Mas(1,10)
Mass(1,11)=Mas(1,11)
Mass(1,12)=Mas(1,12)
Mass(7,7)=Mas(2,2)
Mass(4,7)=Mas(2,3)
Mass(7,10)=Mas(2,4)
Mass(2,7)=Mas(2,5)
Mass(3,7)=Mas(2,6)
Mass(7,8)=Mas(2,7)
Mass(7,9)=Mas(2,8)
Mass(5,7)=Mas(2,9)
Mass(6,7)=Mas(2,10)
Mass(7,11)=Mas(2,11)
Mass(7,12)=Mas(2,12)
Mass(4,4)=Mas(3,3)
Mass(4,10)=Mas(3,4)
Mass(2,4)=Mas(3,5)
Mass(3,4)=Mas(3,6)
Mass(4,8)=Mas(3,7)
Mass(4,9)=Mas(3,8)
Mass(4,5)=Mas(3,9)
Mass(4,6)=Mas(3,10)
Mass(4,11)=Mas(3,11)
Mass(4,12)=Mas(3,12)
Mass(10,10)=Mas(4,4)
Mass(2,10)=Mas(4,5)
Mass(3,10)=Mas(4,6)
Mass(8,10)=Mas(4,7)
Mass(9,10)=Mas(4,8)
Mass(5,10)=Mas(4,9)
Mass(6,10)=Mas(4,10)
Mass(10,11)=Mas(4,11)
Mass(10,12)=Mas(4,12)
Mass(2,2)=Mas(5,5)
Mass(2,3)=Mas(5,6)

```

Mass(2,8)=Mas(5,7)
Mass(2,9)=Mas(5,8)
Mass(2,5)=Mas(5,9)
Mass(2,6)=Mas(5,10)
Mass(2,11)=Mas(5,11)
Mass(2,12)=Mas(5,12)
Mass(3,3)=Mas(6,6)
Mass(3,8)=Mas(6,7)
Mass(3,9)=Mas(6,8)
Mass(3,5)=Mas(6,9)
Mass(3,6)=Mas(6,10)
Mass(3,11)=Mas(6,11)
Mass(3,12)=Mas(6,12)
Mass(8,8)=Mas(7,7)
Mass(8,9)=Mas(7,8)
Mass(5,8)=Mas(7,9)
Mass(6,8)=Mas(7,10)
Mass(8,11)=Mas(7,11)
Mass(8,12)=Mas(7,12)
Mass(9,9)=Mas(8,8)
Mass(5,9)=Mas(8,9)
Mass(6,9)=Mas(8,10)
Mass(9,11)=Mas(8,11)
Mass(9,12)=Mas(8,12)
Mass(5,5)=Mas(9,9)
Mass(5,6)=Mas(9,10)
Mass(5,11)=Mas(9,11)
Mass(5,12)=Mas(9,12)
Mass(6,6)=Mas(10,10)
Mass(6,11)=Mas(10,11)
Mass(6,12)=Mas(10,12)
Mass(11,11)=Mas(11,11)
Mass(11,12)=Mas(11,12)
Mass(12,12)=Mas(12,12)
DO 51, ROW=2,12
  IM1=ROW-1
  DO 51, COL= 1,IM1
    Mass(row,col)=Mass(col,row)
51 continue
end

SUBROUTINE Mass3 (r1,r2,h1,h2,lth,Mass)
INTEGER ROW, COL
REAL Mass(12,12),lth
A1=(r1*h1/10.0)*(26.0*(lth**2) + 7.0*(h1**2))/lth/7.0

```

```

A2 = (r2*h2/10.0)*(26.0*(lth**2)+7.0*(h2**2))/lth/7.0
B1 = (r1*h1/10.0) * (11.0/21.0*(lth**2)+(h1**2)/12.0)
B2 = (r2*h2/10.0) * (11.0/21.0*(lth**2)+(h2**2)/12.0)
C1 = (r1*h1/10.0)*(-9.0*(lth**2)+7.0*(h1**2))/lth/(-7.0)
C2 = (r2*h2/10.0)*(-9.0*(lth**2)+7.0*(h2**2))/lth/(-7.0)
D1 = (r1*h1/10.0)*(-13.0/42.0*(lth**2) + (h1**2)/12.0)
D2 = (r2*h2/10.0) * (-13.0/42.0*(lth**2) + (h2**2)/12.0)
F1 = (r1*h1/10.0) * (2.0/21.0*(lth**3)+(h1**2)*lth/9.0)
F2 = (r2*h2/10.0) * (2.0/21.0*(lth**3)+(h2**2)*lth/9.0)
Z1 = (r1*h1/10.0) * ((lth**3)/(-14.0)-lth*(h1**2)/36.0)
Z2 = (r2*h2/10.0) * ((lth**3)/(-14.0)-lth*(h2**2)/36.0)
U1 = (r1*h1*lth/3.0)
U2 = (r2*h2*lth/3.0)
Mass(1,1)=U1
Mass(1,7)=U1/2.0
Mass(7,7)=U1
Mass(4,4)=U2
Mass(4,10)=U2/2.0
Mass(10,10)=U2
Mass(2,2)=A1
Mass(2,3)=B1
Mass(2,8)=C1
Mass(2,9)=D1
Mass(3,3)=F1
Mass(3,8)=-D1
Mass(3,9)=Z1
Mass(8,8)=A1
Mass(8,9)=-B1
Mass(9,9)=F1
Mass(5,5)=A2
Mass(5,6)=B2
Mass(5,11)=C2
Mass(5,12)=D2
Mass(6,6)=F2
Mass(6,11)=-D2
Mass(6,12)=Z2
Mass(11,11)=A2
Mass(11,12)=-B2
Mass(12,12)=F2
DO 52, ROW=2,12
  IM1=ROW-1
  DO 52, COL= 1,IM1
    Mass(row,col)=Mass(col,row)
52 continue
end

```

APPENDIX 3

Ansys Program

```
/PREP7
/TITLE, SANDWICH BEAM FREE VIBRATION, Non-damping study
KAN,2
ET,1,82
MP,NUXY,1,.3
MP,EX,1,29000000
MP,DENS,1,.000734
N,1,0,0
N,2,0,.125
N,3,0,.25
N,4,0,.3125
N,5,0,.375
N,6,0,.4375
N,7,0,.5
N,8,0,.625
N,9,0,.75
N,10,.238486842,0
N,11,.238486842,.25
N,12,.238486842,.375
N,13,.238486842,.5
N,14,.238486842,.75
NGEN,20,14,1,14,,.476973684
E,1,15,17,3,10,16,11,2
ENGEN,4,19,14,1
EN,4,7,21,23,9,13,22,14,8
ENGEN,4,19,14,4
ET,2,82
MP,EX,2,345.8217
MP,DENS,2,.000115
MP,NUXY,2,.49
MAT,2
EN,2,3,17,19,5,11,18,12,4
EN,3,5,19,21,7,12,20,13,6
ENGEN,4,19,14,2
ENGEN,4,19,14,3
D,1,UY
D,267,UX,,,275
FINISH
```

```
/SOLU  
MODOPT,SUBSP,5  
SOLVE  
FINISH  
/POST1  
SET,LIST  
FINISH
```